

OAK RIDGE  
NATIONAL  
LABORATORY



ORNL/TM-11558



3 4456 0314909 1

### Stellarator Status—1989

- J. F. Lyon
- G. Grieger
- F. Rau
- A. Iiyoshi
- A. P. Navarro
- L. M. Kovrizhnykh
- O. S. Pavlichenko
- S. M. Hamberger

OAK RIDGE NATIONAL LABORATORY  
 CENTRAL RESEARCH LIBRARY  
 CIRCULATION SECTION  
 OAK RIDGE, TENN.  
**LIBRARY LOAN COPY**  
 DO NOT TRANSFER TO ANOTHER PERSON  
 If you wish someone else to see this report, send its name with report and the library will arrange a loan.

OPERATED BY  
MARTIN MARIETTA ENERGY SYSTEMS, INC.  
FOR THE UNITED STATES  
DEPARTMENT OF ENERGY

This report has been reproduced directly from the best available copy.

Available to DOE and DOE contractors from the Office of Scientific and Technical Information, P.O. Box 62, Oak Ridge, TN 37831, prices available from (615) 576-8401, FTS 006-8401.

Available to the public from the National Technical Information Service, U.S. Department of Commerce, 5285 Port Royal Rd., Springfield, VA 22161.

NTIS price codes -- Printed Copy: A03 Microfiche A01

This report was prepared as an account of work sponsored by an agency of the United States Government. Neither the United States Government nor any agency thereof, nor any of their employees, makes any warranty, express or implied, or assumes any legal liability or responsibility for the accuracy, completeness, or usefulness of any information, apparatus, product, or process disclosed, or represents that its use would not infringe privately owned rights. Reference herein to any specific commercial product, process, or service by trade name, trademark, manufacturer, or otherwise, does not necessarily constitute or imply its endorsement, recommendation, or favoring by the United States Government or any agency thereof. The views and opinions of authors expressed herein do not necessarily state or reflect those of the United States Government or any agency thereof.

Fusion Energy Division

## STELLARATOR STATUS—1989

J. F. Lyon

G. Grieger  
F. Rau

Max-Planck-Institut für Plasmaphysik, Garching, Federal Republic of Germany

A. Iiyoshi

National Institute for Fusion Science, Nagoya, Japan

A. P. Navarro

Centro de Investigaciones Energéticas, Medioambientales, y Tecnológicas, Madrid, Spain

L. M. Kovrizhnykh

General Physics Institute of the U.S.S.R. Academy of Sciences, Moscow, U.S.S.R.

O. S. Pavlichenko

Institute of Physics and Technology, Academy of Sciences of the  
Ukrainian SSR, Kharkov, U.S.S.R.

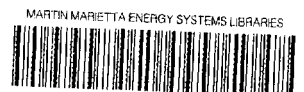
S. M. Hamberger

Plasma Research Laboratory, Research School of Physical Sciences,  
Australian National University, Canberra, Australia

Date Published: July 1990

Prepared for the  
Office of Fusion Energy  
Budget Activity No. AT 10

Prepared by the  
OAK RIDGE NATIONAL LABORATORY  
Oak Ridge, Tennessee 37831-6285  
operated by  
MARTIN MARIETTA ENERGY SYSTEMS, INC.  
for the  
U.S. DEPARTMENT OF ENERGY  
under contract DE-AC05-84OR21400



3 4456 0314909 1



## CONTENTS

ABSTRACT . . . . .	v
1. INTRODUCTION . . . . .	1
2. UNITED STATES . . . . .	2
2.1. The ATF torsatron program . . . . .	2
2.2. University programs . . . . .	6
2.3. ATF-II studies . . . . .	7
2.4. Theory . . . . .	8
3. U.S.S.R. . . . .	9
3.1. Kharkov Institute of Physics and Technology . . . . .	9
3.1.1. Experiment . . . . .	9
3.1.2. Theory . . . . .	11
3.2. Institute of General Physics (Moscow) . . . . .	12
3.2.1. Experiment . . . . .	12
3.2.2. Theory . . . . .	13
4. JAPAN . . . . .	14
4.1. CHS (National Institute for Fusion Science) . . . . .	14
4.2. Plasma Physics Laboratory, Kyoto University . . . . .	16
4.2.1. Heliotron E . . . . .	16
4.2.2. Heliotron DR . . . . .	17
4.3. TU-Heliac (Tohoku University) . . . . .	18
4.4. SHATLET-M (University of Tokyo) . . . . .	18
4.5. The LHD project (National Institute for Fusion Science) . . . . .	18
4.6. Theory and computation . . . . .	20
5. AUSTRALIA . . . . .	21
6. EUROPEAN COMMUNITY . . . . .	23
6.1. The TJ-II flexible heliac project . . . . .	24
6.2. TJ-I Upgrade . . . . .	25
6.3. Wendelstein VII-AS . . . . .	25
6.4. The Wendelstein VII-X project . . . . .	27
6.5. Theory . . . . .	29
7. SUMMARY . . . . .	30
ACKNOWLEDGMENTS . . . . .	31
REFERENCES . . . . .	32



**ABSTRACT**

The present status of stellarator experiments and recent progress in stellarator research (both experimental and theoretical) are reported by groups in the United States, the U.S.S.R., Japan, Australia, and the European Community (the Federal Republic of Germany and Spain). Experiments under construction and studies of large, next-generation stellarators are also described.



## 1. INTRODUCTION

Stellarators belong to the family of toroidal magnetic confinement devices, along with tokamaks and reversed-field pinches (RFPs). This family is characterized by toroidally closed, nested magnetic surfaces produced by helical magnetic fields with toroidal and poloidal components. The confining poloidal field is produced by currents in external windings in a stellarator and by a net plasma current in tokamaks and RFPs. The similarities in physics and technology that stellarators share with tokamaks have allowed stellarators to achieve plasma performance at least comparable to that obtained in tokamaks of similar scale. In addition, stellarators have some distinct and advantageous differences that favor their development as economical fusion reactors [1].

The recent substantial progress in plasma parameters, physics understanding, and stellarator concept improvement has been covered in previous assessments of the field [1, 2] and continues in both theory and new experiments [3]. Experiments have been successful not only in extending plasma parameters but also in extracting important information about the effects of shear, trapped particles, electric fields, resonances, and magnetic islands. Significant progress has been made in developing detailed theoretical understanding of equilibrium, stability, and transport properties. In combination with the availability of more powerful codes and computers, this has increased the reliability of theoretical predictions of higher beta limits, the second stability region, the beneficial influence of a helical axis on stability, the effect of electric fields on transport, the reduction of secondary currents, the effects of the bootstrap current, etc.

The confinement potential [particle orbits, neoclassical transport, magneto-hydrodynamic (MHD) equilibrium and stability behavior, bootstrap current, etc.] of stellarators depends on the properties of the magnetic configuration, including rotational transform  $\iota$ , shear, magnetic well or hill, field ripple, helical axis excursion, and reduction of secondary currents (reduced poloidal variation of  $\int dl/B$ ) [1]. Four characteristic stellarator lines based on different optimization principles are being studied in present and near-term experiments:

- (1) High-transform, high-shear stabilized configurations (heliotrons) are being investigated by the Heliotron group (Kyoto, Japan).
- (2) Moderate-transform, shear/magnetic-well stabilized configurations (tor-satrons) with access to the second stability regime are being studied by the Advanced Toroidal Facility (ATF) group (Oak Ridge, Tennessee, U.S.A.) and by groups in the U.S.S.R. and Japan.
- (3) Moderate-transform, low-shear, magnetic-well stabilized,  $\delta \int dl/B$ -reduced, drift-optimized configurations (Advanced Stellarators) are being explored by the Wendelstein group [Garching, Federal Republic of Germany (FRG)].
- (4) High-transform, low-shear, magnetic-well stabilized configurations with large helical excursions of the magnetic axis (heliacs) are being pursued by groups in Australia, Japan, and Spain.

A new generation of larger experiments to demonstrate the potential of the stellarator concept is now under design: Wendelstein VII-X at Garching would combine elements of approaches (3) and (4), the Large Helical Device (LHD) at the National Institute for Fusion Science in Nagoya would combine elements of approaches (1) and (2), and ATF-II at Oak Ridge would extend approach (2) to lower aspect ratio. The complementary approaches in the present and next-generation experiments are designed to establish the relative importance of the different magnetic field properties in configuration optimization.

This report summarizes the status of these present and near-term experiments and recent progress in stellarator research by the various groups. Fourteen stellarator experiments are operating in the United States, the U.S.S.R., Japan, Australia, and countries of the European Community, and five more are under construction. Three of the larger experiments began operation in 1988, and three of the experiments under construction are scheduled to begin operation in 1990. The main characteristics of the operating stellarators are listed in Table I; those of the stellarators under construction, in Table II.

## 2. UNITED STATES

The main component of the U.S. program is the ATF [4], currently the world's largest stellarator, at Oak Ridge National Laboratory (ORNL). In addition, a small university experimental program is studying basic elements of stellarator physics, and there is a strong theoretical effort at several institutions.

### 2.1. ATF

ATF is a moderate-aspect-ratio,  $\ell = 2$ ,  $M = 12$  torsatron with major radius  $R_0 = 2.1$  m, average plasma radius  $\bar{a} = 0.27$  m, and on-axis field  $B_0 = 2$  T for a 5 s pulse. Here  $\ell$  is the poloidal multipolarity of the field and  $M$  is the number of toroidal field periods. For plasma production and heating, ATF uses 0.4 MW, 53 GHz electron cyclotron heating (ECH); 2 MW, 40 kV  $H^0$  neutral beam injection (NBI); and 0.3 MW, 5 to 16 MHz ion cyclotron heating (ICH). Operation started in January 1988. The first year of operation [5] included electron-beam mapping of the vacuum flux surfaces; analysis and correction of some resonant low-order field perturbations; study of second stability behavior; studies of plasma heating with ECH, NBI, and ICH at  $B_0 = 1$  T; density control with gas puffing and impurity control with chromium gettering; studies of plasma collapse behavior with NBI; and confinement scaling studies. During the second year of operation (1989), studies of plasma heating and confinement scaling were extended to higher parameters at  $B_0 = 2$  T with additional vertical field shaping, pellet injection, titanium gettering, and additional diagnostics. Experiments focused on plasma performance optimization; the dependence of the measured bootstrap current on plasma pressure,

TABLE I. DEVICE PARAMETERS FOR OPERATING STELLARATORS

Name	Location	Type <sup>b</sup>	Parameter <sup>a</sup>						
			$\ell$	M	$R_0$ (m)	$\bar{a}$ (m)	$B_0$ (T)	Heating power (MW); type <sup>c</sup>	Start Date
ATF	Oak Ridge, USA	T	2	12	2.1	0.27	2.0	2.7; N,E,I	1988
Proto-CLEO	Madison, USA	S, T	3	7	0.4	0.04	0.3	0.1; I	1975
IMS	Madison, USA	MS	3	7	0.4	0.04	0.8	0.02; E	1984
AT	Auburn, USA	T	2	10	0.58	0.1	0.2	0.05; I,E	1984
HBQM	Seattle, USA	LS/H	1	7.5	—	0.1	0.4	$\theta$ -pinch	1984
Uragan-3, -3M	Kharkov, USSR	T	3	9	1.0	0.11	2	0.6; I	1981
L-2	Moscow, USSR	S	2	14	1.0	0.115	1.3	0.48; E,O	1975
CHS	Nagoya, Japan	H/T	2	8	1.0	0.2	1.5	1.4; N,I,E	1988
Heliotron E	Uji, Japan	H/T	2	19	2.2	0.2	2.0	7; N,I,E	1980
Heliotron DR	Uji, Japan	H/T	2	15	0.9	0.07	0.6	0.2; E	1981
TU-Heliac	Sendai, Japan	H		4	0.48	0.1		$5 \times 10^{-4}$ ; E	1988
SHATLET-M	Tokyo, Japan	MT	2	12	0.42	0.05	0.15	300-J laser	
SHEILA	Canberra, Australia	H		3	0.2	0.03	0.3	0.005; I,E,A	1984
W VII-AS	Garching, FRG	MS		5	2.0	0.2	2.5	5.5; I,N,E	1988

<sup>a</sup> $\ell$  = poloidal multipolarity of the field,  $M$  = number of toroidal periods,  $R_0$  = major radius,  $\bar{a}$  = average plasma radius,  $B_0$  = on-axis magnetic field.

<sup>b</sup>T = torsatron, S = stellarator, MS = modular stellarator, LS/H = linear stellarator/heliac, H/T = heliotron/torsatron, MT = modular torsatron, H = heliac.

<sup>c</sup>N = neutral beam injection, I = ion cyclotron heating, E = electron cyclotron heating, O = Ohmic heating, A = ac Ohmic heating; order indicates decreasing power.

TABLE II. DEVICE PARAMETERS FOR STELLARATORS UNDER CONSTRUCTION

Name	Location	Type <sup>b</sup>	Parameter <sup>a</sup>							Start Date
			$\ell$	M	$R_0$ (m)	$\bar{a}$ (m)	$B_0$ (T)	Heating power (MW); type <sup>c</sup>		
CAT	Auburn, USA	T	2,1	5	0.53	0.11	0.1	0.06; I,E	1990	
Uragan-2M	Kharkov, USSR	T	2	4	1.7	0.22	2.4	8.5; I,N	1991	
H-1	Canberra, Australia	H		3	1.0	0.22	1.0	0.2; I	1990	
TJ-II	Madrid, Spain	H		4	1.5	0.2	1.0	0.4; E	1994	
TJ-I Upgrade	Madrid, Spain	T	1	6	0.6	0.1	0.5	0.2; E	1990	

<sup>a</sup> $\ell$  = poloidal multipolarity of the field,  $M$  = number of toroidal periods,  $R_0$  = major radius,  $\bar{a}$  = average plasma radius,  $B_0$  = on-axis magnetic field.

<sup>b</sup>T = torsatron, S = stellarator, MS = modular stellarator, LS/H = linear stellarator/heliac, H/T = heliotron/torsatron, MT = modular torsatron, H = heliac.

<sup>c</sup>N = neutral beam injection, I = ion cyclotron heating, E = electron cyclotron heating; order indicates decreasing power.

field strength, and poloidal field shaping; characterization of fluctuations near the plasma edge; and impurity studies.

Evidence for beta self-stabilization (second stability) has been obtained in ATF [6]. On-axis beta values [ $\beta(0) \leq 3\%$ ] are well above the theoretical value [ $\beta(0) \simeq 1.3\%$  for ideal modes] for transition to the second stability regime for the peaked pressure profiles obtained in ATF. Coherent  $n = 1$  poloidal magnetic fluctuations ( $\tilde{B}_\theta$ ) are observed to first increase with beta and then decrease at higher values, as shown in Fig. 1. Single-helicity calculations of the saturated level of  $\tilde{B}_\theta$  for resistive interchange modes show this same beta dependence. Multiple-helicity calculations of the saturated mode spectrum in toroidal geometry give  $m = 2, n = 1$  and  $m = 3, n = 1$  for the dominant components, as in the experiment. Here  $m$  and  $n$  are the poloidal and toroidal mode numbers, respectively. The pressure profile broadens with beta, similar to the calculated radial expansion of the magnetic well region that produces second stability in stellarators. Theoretical calculations that incorporate this profile broadening indicate that the plasma follows the path of ideal MHD marginal stability into the second stability regime.

Although 1 s operation was obtained on ATF with ECH, a collapse of the plasma stored energy (and then the plasma density) was observed with NBI during the first year of operation. In 1989, 2 MW NBI and  $\simeq 60\%$  coverage with titanium gettering at  $B_0 = 1.9$  T allowed operation with the full 0.25 s NBI pulse length and delay of the thermal collapse; stored energies of 28 kJ; a line-averaged density  $\bar{n}_e = 9 \times 10^{19} \text{ m}^{-3}$  with injection of  $1.2 \text{ km}\cdot\text{s}^{-1}$ , 0.9 mm diam hydrogen pellets;

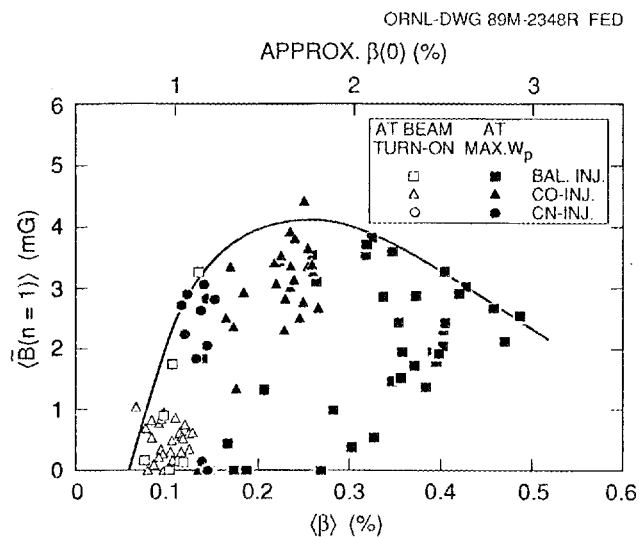


Fig. 1. Variation of the maximum amplitude of coherent  $n = 1$  magnetic oscillations with increasing beta in ATF, indicating a beta self-stabilization effect and entrance to a second stability region.

and energy confinement time  $\tau_E = 20$  ms. A volume-average beta  $\langle\beta\rangle$  of 0.84% was obtained with pellet injection at  $B_0 = 0.95$  T. By early 1990, plasma parameters had further increased:  $\langle\beta\rangle$  to 1.5% at  $B_0 = 0.63$  T,  $\bar{n}_e$  to  $1.2 \times 10^{20}$  m $^{-3}$ ,  $\tau_E$  to 25 ms (with 1.2 MW NBI), plasmas with durations of 0.35 s with NBI that were quasi-stationary for 0.2 s and showed little sign of evolution toward a collapse (limited only by NBI pulse length), and plasma durations of 3.2 s with ECH alone.

Confinement scaling studies [7] on ATF with ECH and NBI-heated plasmas indicate general agreement with the LHD scaling [8];  $\tau_E$  improves with higher  $B_0$  and  $\bar{n}_e$  and decreases with higher heating power. Although the ion confinement appears to be neoclassical, the electron confinement is anomalous. The toroidal current observed during ECH is predominantly bootstrap current and ranges between +3 kA and -1 kA. The observed current agrees with neoclassical theory in magnitude (to within 30%) and parametric dependences as determined by systematic scans of the quadrupole and dipole vertical fields and of the helical field intensity. These results show that the neoclassical theory of bootstrap current accurately describes the plasma current in ATF despite the presence of anomalies in particle and heat flows (as indicated by steady-state particle and power balance studies).

Fast reciprocating Langmuir probe measurements of turbulence near the plasma edge ( $\bar{r} > 0.95\bar{a}$ ) show fluctuating potential ( $\tilde{\phi}$ ) and fluctuating density ( $\tilde{n}_e$ ) levels  $e\tilde{\phi}/kT_e > \tilde{n}_e/n_e$  with poloidal wavelengths  $\lambda_\theta = 0.015$ -0.06 m and phase velocities  $v_{ph} \sim 10^3$  m·s $^{-1}$  in the electron diamagnetic direction [9]. Here  $T_e$  is the local electron temperature. The edge fluctuation levels are typically  $\tilde{n}_e/n_e \simeq 0.05$ -0.1 and  $e\tilde{\phi}/kT_e \simeq 0.1$ -0.2; the difference between these quantities increases with distance into the plasma. The general features are consistent with those found in the Texas Experimental Tokamak (TEXT); the leading candidate is coupling of resistive electrostatic turbulence with a radiative thermal instability. The measured fluctuation-induced edge flux is comparable to that obtained from global particle balance and that estimated from Bohm diffusion. Local measurements of the density fluctuation spectra in ECH plasmas with a two-frequency reflectometer agree with the Langmuir probe measurements at the edge.

## 2.2. University programs

Small experimental programs are carried out at the University of Wisconsin (Madison), Auburn University, and the University of Washington (Seattle). Basic studies have been conducted at the University of Wisconsin on the Proto-CLEO stellarator and torsatron experiments and on the newer Interchangeable Module Stellarator (IMS) [10] with  $R_0 = 0.4$  m,  $\bar{a} \simeq 0.04$  m, and  $B_0 = 0.8$  T. Stochastic heating models have been successfully applied to the breakdown and discharge dynamics of ECH experiments on IMS and have demonstrated the importance of magnetic saddle points in a stellarator topology [11]. Steady-state hollow density

profiles, observed over a wide range of ECH conditions, are accurately modeled with a convective term in the particle balance equation. Poloidal electric fields have been shown to be important in driving this convection [12]. The ability to alter and control diverted particle fluxes through the use of externally applied electric and magnetic fields has also been demonstrated.

Experiments at Auburn University on the Auburn Torsatron ( $R_0 = 0.58$  m,  $\bar{a} = 0.1$  m,  $B_0 = 0.2$  T) have focused on comparative studies of field mapping techniques, use of resonant helical windings to correct field errors, and development of an electron cyclotron emission diagnostic for ATF. A new device, the Compact Auburn Torsatron ( $R_0 = 0.53$  m,  $\bar{a} = 0.11$  m,  $B_0 = 0.1$  T), now under construction, will have both  $\ell = 1$  and  $\ell = 2$  windings for study of magnetic islands, field error correction, and magnetic configuration optimization.

The High-Beta Q-Machine (HBQM) at the University of Washington is a 3 m long, 0.2 m diam, 15 to 30 kJ linear theta pinch with a center hardcore current that has been used for studies of the high-beta ( $\langle\beta\rangle = 30\%$ ) equilibrium of  $\ell = 1$  stellarators and heliacs. Typical plasma parameters are  $n_e \simeq (0.5-1) \times 10^{21}$  m<sup>-3</sup>, electron and ion temperatures  $T_e + T_i \simeq 80-100$  eV, and  $\tau_E \sim 10-15$   $\mu$ s. Large-aspect-ratio toroidicity effects that break the helical symmetry can be simulated by shifting the hardcore conductor from the  $\ell = 1$  stellarator axis.

### 2.3. ATF-II studies

Scoping studies for a large, next-generation stellarator, ATF-II [13], have been conducted at ORNL. These studies include physics constraints (beta limits, transport, orbit confinement, and plasma-wall separation), engineering optimization (cost, access, and high-current-density superconducting windings), and reactor feasibility (transport,  $\alpha$ -particle confinement, shielding, and blankets). The most developed option for ATF-II, the  $M = 6$  Compact Torsatron shown in Fig. 2, has as design parameters  $R_0 = 2$  m,  $\bar{a} = 0.52$  m, and 10 to 15 MW of heating power. High-current-density, high-field, cable-in-conduit NbTi/Cu superconductor would allow adequate plasma-wall separation ( $>0.15$  m), large access ports ( $\simeq 2$  m  $\times$  1 m), and an adequate stability margin ( $\sim 10^5$  J·m<sup>-3</sup>) for steady-state operation at  $B_0 = 4$  T with 4.2 K helium cooling or  $B_0 = 5$  T with 2.5 K helium cooling.

Such a device would be comparable in scope to other next-generation stellarators [3] but would have roughly the same aspect ratio as the mainstream tokamaks. A major motivation for adopting this approach is to reduce the cost of a later stellarator deuterium-tritium (D-T) demonstration device. The primary goal of ATF-II would be to study some of the key issues relating to the feasibility of stellarators as attractive steady-state reactors: high-beta, steady-state operation; confinement at low collisionality; loss of energetic helically trapped particles; particle and impurity control; plasma heating and heat removal; endurance of wall materials and in-vessel components; and integration of superconducting coils in a working experiment.

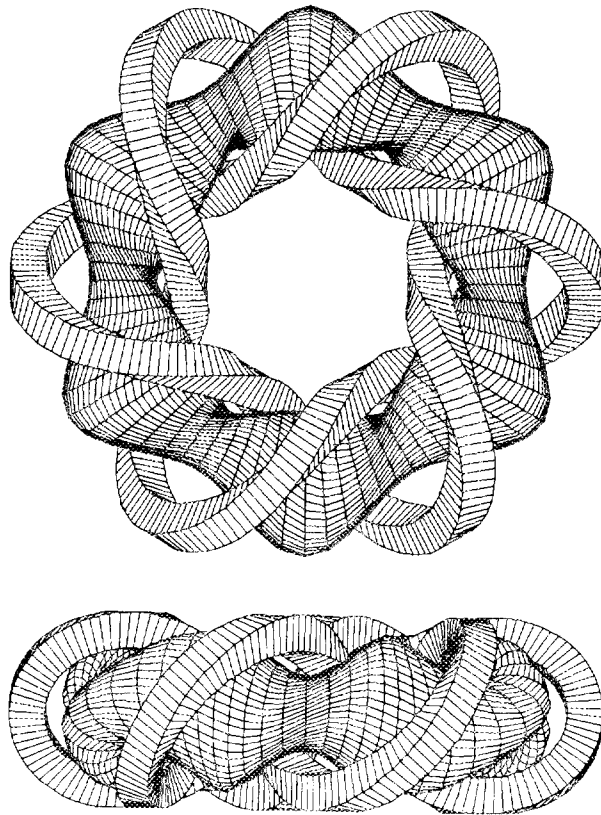


Fig. 2. The helical windings and the last closed flux surface for an  $M = 6$  ATF-II.

In reactor scoping studies [14], minimum-size ( $R_0 = 8\text{--}11$  m) Compact Torsatron reactors have been examined for performance,  $\alpha$ -particle confinement, and shielding and blanket requirements and for practicality as a medium-size ( $R_0 \simeq 4$  m) copper-coil ignition experiment. Despite considerable predicted  $\alpha$ -particle losses [15], the low-aspect-ratio Compact Torsatron approach appears attractive. An integrated optimization approach has yielded configurations with better confinement properties at high beta than projected for ATF or the Compact Torsatrons, but an attractive coil set to create these configurations needs to be developed.

#### 2.4. Theory

Studies in the United States span the entire range of stellarator theory, and U.S.-developed theory and codes are widely used for studies of MHD equilibrium and stability, neoclassical and anomalous transport, radial electric fields, bootstrap currents, and rf power deposition [16].

Computational tools for magnetic field design and MHD equilibrium and stability applications have been improved significantly, with both two-dimensional (2-D) and three-dimensional (3-D) codes being developed, coupled to each other, and used for improvement of basic understanding of plasma confinement, for analysis of existing experiments, and for design studies related to future devices. The prediction and subsequent experimental demonstration of second stability operation in ATF represent a good illustration of the efficacy of these tools. Magnetic coordinates are being used to study the nature of magnetic islands in 3-D configurations and to develop techniques to control their size.

In the single-particle confinement and transport area, a fairly complete theory of neoclassical transport has been developed; it includes the effects of the ambipolar radial electric field and predicts the bootstrap current measured in ATF. This is especially important for low-aspect-ratio devices, in which the effect of particle trapping in the helical wells must be considered. Monte Carlo codes of various types have been used to estimate particle diffusivities and confinement times, and Fokker-Planck codes (bounce-averaged or using the full guiding-center distribution) have been used to calculate the different elements of the transport matrix. One-dimensional transport codes have been used to predict and analyze performance in stellarators. The effect of electric fields on neoclassical transport and on reduction of anomalous transport has been studied. Models of anomalous transport driven by turbulence associated with resistive pressure-driven interchange instabilities appear to agree with experiment. Study of the dissipative trapped electron mode has identified features that should allow this mode to be more easily identified in stellarators than in tokamaks. Ray tracing techniques and full-wave calculations have improved our ability to predict the deposition of energy by ECH and ICH in 3-D configurations. Plasma behavior in the divertor region has also been studied extensively.

### 3. U.S.S.R.

Stellarator research in the U.S.S.R. is primarily conducted at the Kharkov Institute of Physics and Technology (Uragan-3 and Uragan-2M) and at the Institute of General Physics (L-2) in Moscow, formally part of the Lebedev Institute. In addition, there are smaller stellarator theory efforts at the Kurchatov Institute of Atomic Energy and at other laboratories.

#### 3.1. Kharkov Institute of Physics and Technology

##### 3.1.1. *Experiment*

The Uragan-3 torsatron [ $\ell = 3$ ,  $M = 9$ ,  $R_0 = 1$  m,  $\bar{a} = 0.085$  m,  $B_0 < 1$  T, rotational transform on axis  $\iota(0) = 0$ , edge rotational transform  $\iota(\bar{a}) = 0.3$ ] [17]

has been used for studies of rf plasma production and heating in a stellarator geometry with an open helical divertor (magnetic field windings inside a large vacuum chamber). Currentless plasmas were created by excitation of ion cyclotron waves and Alfvén waves in the plasma with helical frame antennas. Optimization studies resulted in quasi-stationary (Q) discharges (duration  $> 50$  ms) with high ion temperature [ $T_i(0) \simeq 1.1$  keV] and high beta [ $\beta(0) \simeq 1\%$ ] for rather small rf power absorbed ( $P_{\text{abs}} \simeq 11$  kW) in a low-density plasma ( $\bar{n}_e \simeq 2 \times 10^{18} \text{ m}^{-3}$ ). Such regimes are realized when most ( $\simeq 90\%$ ) of the rf power radiated by the antenna goes to creating a low-density cold plasma mantle in the whole vacuum chamber (volume =  $70 \text{ m}^3$ ). The rf power absorbed by the plasma mostly goes to heating the electrons [ $T_e(0) = 0.3$  keV] and is lost equally by electron heat conduction and radiation (10 kW total). The ion energy losses are mostly by charge exchange (1 kW). Comparison of experimental data with theoretical predictions showed that the electron heat diffusivity  $\chi_e$  is consistent with neoclassical values at the plasma center and is anomalous ( $\chi_e \simeq 10^{19} n_e^{-1} T_e^{-2/3} \text{ m}^2 \cdot \text{s}^{-1}$ ) at the edge ( $\bar{r} = 0.7\bar{a}$ ) [18]. The light impurity content is rather small ( $n_{\text{C,O}} < 1\%$ ) in Q-discharges, and the radiative losses arise from metal impurities coming from the helical winding casings. A carbon injection experiment allowed estimation of the particle diffusivity ( $D \simeq 1.4 \text{ m}^2 \cdot \text{s}^{-1}$ ) and the inward flow velocity ( $v \simeq 35 \text{ m} \cdot \text{s}^{-1}$ ) [19]. A relaxation instability, analogous to that observed in currentless high-beta Heliotron E plasmas, has been observed in Q-discharges with  $\beta(0) > 0.6\%$ , as shown in Fig. 3 [20].

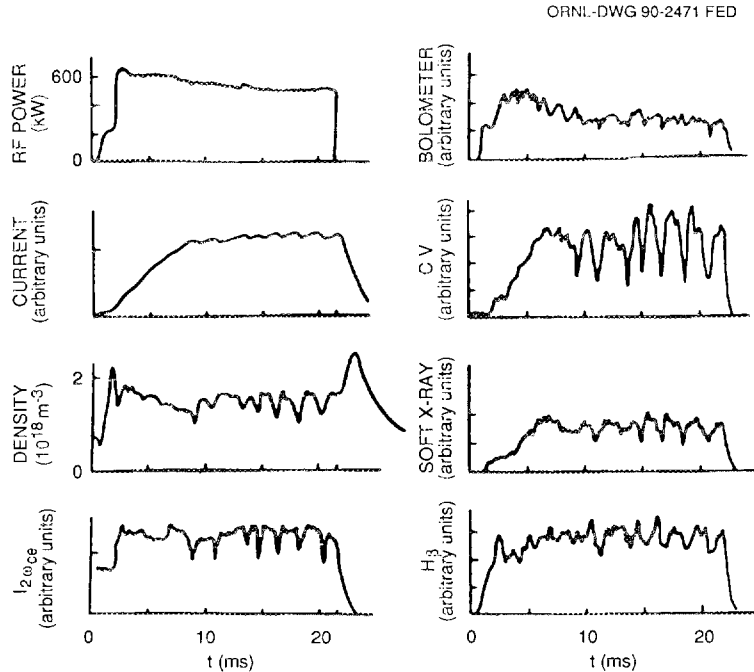


Fig. 3. Relaxation oscillations in plasma parameters in an Uragan-3 Q-discharge ( $B_0 = 0.43$  T,  $B_V/B_0 = 0.48\%$ ).

New helical windings with the same dimensions as the old windings, but able to operate at higher magnetic field (up to 2 T), and two additional inner vertical field coils were installed in 1989 on Uragan-3, which was then renamed Uragan-3M. Magnetic surface mapping studies using emissive diode and luminescent rod techniques showed that the average radius of the last closed magnetic surface increased from 0.085 m to 0.11 m. Variation of the vertical field should allow study of both magnetic-hill and magnetic-well configurations and their influence on plasma stability. Experimental studies resumed in March 1990.

Construction of a new device, Uragan-2M [ $R_0 = 1.7$  m,  $\bar{a} = 0.22$  m,  $B_0 = 2.4$  T,  $\ell = 2$ ,  $M = 4$ ,  $\epsilon(0) = 0.2\text{--}0.57$ ,  $\epsilon(\bar{a}) = 0.75$ ] [21], a torsatron with an additional toroidal field, is continuing. All major device components (except the helical windings) have been received; start of operation is projected for March 1991. The main advantage of this torsatron design is the reduction of the helical ripple of the magnetic field at modest values of rotational transform and shear. High-power systems (7 MW ICH, 1.5 MW NBI) for plasma production and heating should allow study of beta limits and collisionless plasma confinement.

### 3.1.2. Theory

Plasma equilibrium current control and neoclassical transport are the main areas of stellarator theory activity. The main results are as follows.

- (1) The Pfirsch-Schlüter current can be reduced in a torsatron by a proper choice of helical winding modulation when the slope of the helical windings is shallow on the inside of the torus. For a torsatron with a low aspect ratio ( $R_0/\bar{a} \simeq 3.5$ ),  $M = 8$ , and  $\ell = 2$ ,  $j_{\parallel}(r)$  may be diminished by a factor of 1.5–2.4. This effect follows from the analytical expression for  $j_{\parallel}$ , where in addition to the standard factor  $\propto 1/\epsilon$ , terms proportional to the Fourier coefficients of satellite harmonics with controllable signs appear. The reduction of Pfirsch-Schlüter currents occurs when the helical ripples are localized on the high-field side of the torus [22]. Reduction of plasma equilibrium currents leads to smaller transverse magnetic fields ( $\propto \beta$ ) and consequently to less destruction of magnetic surfaces [23].
- (2) At finite plasma pressure, as with the vacuum configuration, proper choice of the modulation coefficient of the helical winding trajectory can reduce neoclassical transport in the  $1/\nu$  regime by nearly half [24]. Here  $\nu$  is the collision frequency. This reduction, analytically predicted in earlier work, is confirmed by a Monte Carlo simulation. Here  $D(\nu)$  does not increase at intermediate values of  $\nu$ , as is typical in usual stellarators [25].

## 3.2. Institute of General Physics (Moscow)

### 3.2.1. Experiment

The L-2 stellarator ( $R_0 = 1$  m,  $\bar{a} = 0.115$  m,  $\ell = 2$ ,  $M = 14$ ) [26] has been used for studies of plasma production and heating both at the electron cyclotron fundamental frequency ( $f = f_{ce} = 37.5$  GHz) and at its second harmonic ( $f = 2f_{ce} = 75$  GHz) for  $B_0 = 1.33$  T. The gyrotron power was 200 kW at the fundamental frequency and 280 kW at the second harmonic, with a pulse duration of 8–9 ms. Microwave power was launched from the low-field side in both cases using a quasi-optical mirror system to form a Gaussian beam with a diameter of 0.065 m in the absorption region. The second harmonic wave had extraordinary mode (X-mode) polarization, and the fundamental wave had ordinary mode (O-mode) polarization. When an O-mode wave at the fundamental frequency was used, a plasma was obtained with  $\bar{n}_e = 9 \times 10^{18}$  m $^{-3}$ , thermal energy  $W = 200$  J,  $T_e(0) \simeq 800$ –1000 eV, and  $\tau_E \simeq 3.5$  ms, with 40–50% of the microwave power absorbed in the plasma [27]. In the second harmonic X-mode experiment, the plasma energy reached as much as 400 J, with  $\bar{n}_e \simeq 1.35 \times 10^{19}$  m $^{-3}$  and  $T_e(0) \simeq 1000$ –1100 eV. In this case almost all of the power (90–100%) was absorbed. Ray tracing calculations carried out for a one-pass model resulted in an absorption coefficient close to that obtained experimentally.

A nonlinear dependence of  $T_e(0)$  on power  $P$  was inferred from the experiment in the range  $P = 100$ –260 kW, namely  $T_e \propto P^\alpha$ , where  $\alpha = 0.35$ –0.4. The energy confinement time  $\tau_E = 1.5$ –2 ms at  $P = 280$  kW [28]. According to estimates based on the neoclassical heat transport model, the plasma electron component is in the low-collisionality regime where the heat conduction is  $\propto 1/\nu$ . This is apparently the reason for the weak dependence of  $T_e(0)$  on  $P$  and the decrease in  $\tau_E$ . In the near future, ECH plasma experiments are planned with  $f = 2f_{ce}$  and with the microwave power increased to 700–800 kW with a pulse duration of 20 ms. This should allow study of the dependences of  $T_e$  and of  $W$  on  $P$  over a wider range of  $P$  for nearly stationary plasma conditions.

Density fluctuation spectra were inferred from the measured spectrum of a scattered 2 mm wavelength probing beam. The fluctuations appeared to have the characteristics of drift waves and had relative amplitudes  $\delta n_e/n_e \sim 5$ –15% [29]. A correlation was established between  $T_e(0)$  and  $\delta n_e/n_e$ ;  $T_e(0)$  increases with decreasing  $\delta n_e/n_e$ , as shown in Fig. 4.

Values of  $\beta(0)$  as high as 0.5% were obtained in the X-mode experiment, which is enough to modify the magnetic structure near the center of the plasma column such that the magnetic axis shifts by some centimeters. The asymmetry of the electron temperature profile, inferred from soft X-ray measurements, that appears when beta increases provides some evidence for this displacement.

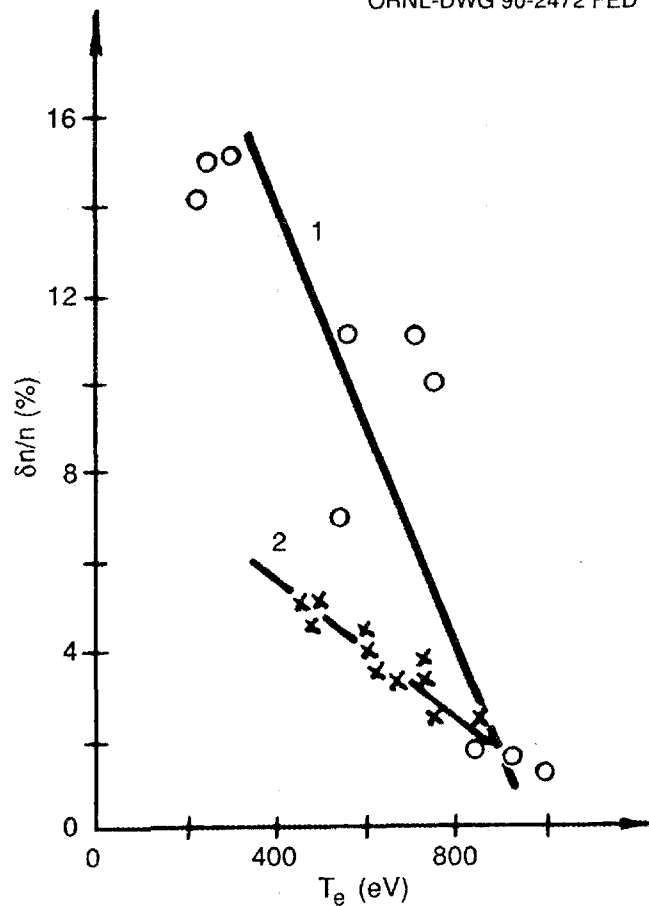


Fig. 4. Correlation of density fluctuation level with central electron temperature in L-2 for (1) 170 kW ECH hydrogen plasmas and (2) 100 kW ECH helium plasmas.

### 3.2.2. Theory

The main fields of study were

- (1) more detailed work on neoclassical heat conduction effects;
- (2) the beta limit and the magnetic structure of the plasma (equilibrium bifurcation with formation of magnetic islands);
- (3) stellarator optimization and acceptable next-generation machines;
- (4) related problems [ $\alpha$ -particle confinement, more precise models for calculation, participation in studies of stellarator reactors (with the Efremov Institute, Leningrad)].

The following results were obtained:

- (1) Analysis of particle confinement in a torsatron with a large number of trapped-detrapped orbits (when the helical parameter  $\epsilon_H$  is comparable with the

toroidal parameter  $\epsilon_T$ ) showed that another maximum can appear in the transport coefficients  $D(\nu)$  and  $\chi(\nu)$  at a  $\nu$  value below the superbanana maximum. Earlier results on this subject obtained by other authors were generalized and some errors corrected [30, 31]. The earlier results appear to correspond to particular values of a parameter proportional to the ratio of the times in which the particles are in the trapped and detrapped states.

- (2) The possibility of plasma equilibrium bifurcation with formation of magnetic islands was found when beta increased. The most general conditions for bifurcation were determined for the ideal MHD model by assuming that the plasma boundary and the functional dependence of the pressure profile are fixed [32].
- (3) A stellarator concept was developed with optimized neoclassical heat and particle diffusivity and with sufficient stabilizing shear [33].
- (4) With the Efremov Institute, solutions of the neoclassical heat and particle balance equations were studied. It was shown that rather rigid control of the heat and particle source functions is needed to obtain a stationary plasma profile under reactor conditions [34].

## 4. JAPAN

Helical systems research in Japan is primarily conducted at the new National Institute for Fusion Science [the Compact Helical System (CHS) and the proposed LHD] and at the Kyoto University Plasma Physics Laboratory (Heliotron E and Heliotron DR). Smaller research efforts are located at Tohoku University (TU-Heliac) and at the University of Tokyo (SHATLET-M).

### 4.1. CHS (National Institute for Fusion Science)

The main objective of CHS [35] is to establish an experimental data base on low-aspect-ratio plasmas for the design of next-generation devices. CHS has been in operation since April 1988. Experiments with 28 GHz and 53 GHz ECH have been performed at  $B_0 \simeq 1$  T and with heating powers of <150 kW each. The density range for these experiments is  $(2-20) \times 10^{18} \text{ m}^{-3}$ , and the electron temperature is 200-1200 eV. Fundamental resonance ECH experiments with the 53 GHz gyrotron are not yet possible because the present power supply limits the magnetic field strength ( $B_0 \leq 1.5$  T). The first neutral beam injector was installed in March 1989. Its injection angle can be scanned from tangential to perpendicular for the purpose of varying the pitch angle of the injected ions. Tangential co-injection experiments started in June 1989 with a beam voltage of 40 kV. Various schemes for target plasma production with ECH and ion cyclotron range of frequencies (ICRF) power

were used at  $B_0 = 0.46\text{--}1.5$  T. The electron and ion temperatures are  $T_e = 200\text{--}600$  eV and  $T_i = 200\text{--}400$  eV for the density range  $(1\text{--}10) \times 10^{19} \text{ m}^{-3}$ . The stored energy measured with a diamagnetic loop ( $W_{\text{dia}}$ ) is up to 5.4 kJ.

Confinement characteristics have been studied [36]: the dependence of the global energy confinement time  $\tau_E^{\text{exp}}$  on  $B_0$ ,  $\bar{n}_e$ , deposited power  $P_{\text{in}}$ , and magnetic axis position  $R_{\text{axis}}$ . The confinement time  $\tau_E^{\text{exp}}$  is defined as  $W_{\text{dia}}$  divided by  $P_{\text{in}}$ , which is estimated analytically for both ECH and tangential NBI plasmas. Estimated absorption rates for the port-through power are 70–90% for NBI plasmas and up to 80% for ECH plasmas. The decay of electron temperature after the ECH power is turned off has been measured with Thomson scattering. The experimental results show that the ECH power deposition is fairly well localized to the core region, which is consistent with an analytic estimate. Monte Carlo calculation of NBI to estimate the power deposition profile and the loss of high-energy ions during their thermalization has not been done yet.

Figure 5 shows that  $\tau_E^{\text{exp}}$  roughly follows the LHD scaling [8]; the LHD scaling is pessimistic in the low- to medium-density regime ( $\bar{n}_e < 4 \times 10^{19} \text{ m}^{-3}$ ) and optimistic for high densities ( $\bar{n}_e > 5 \times 10^{19} \text{ m}^{-3}$ ). Radiation loss usually increases as the density increases; in some cases, more than 60% of the port-through

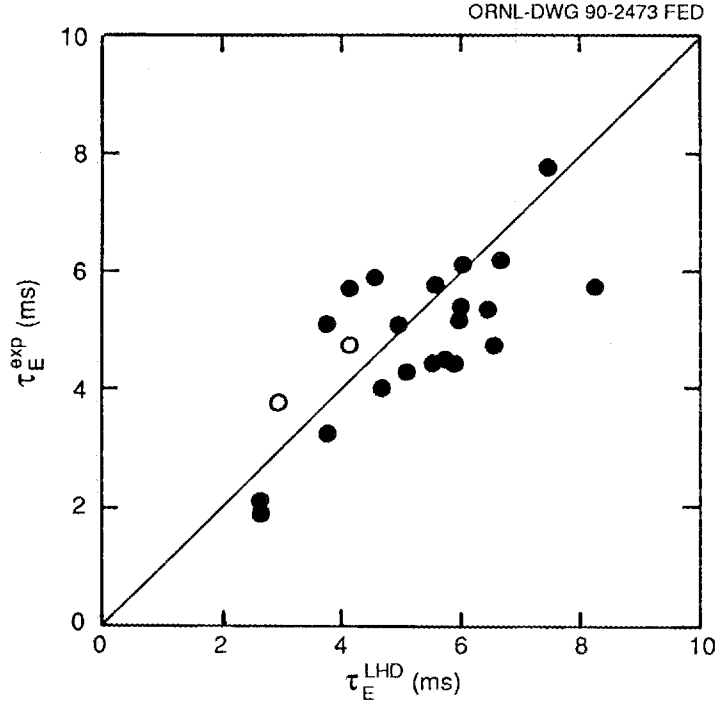


Fig. 5. Comparison of  $\tau_E^{\text{exp}}$  in CHS with the LHD scaling. Solid circles: NBI plasmas. Open circles: ECH plasmas.  $\bar{n}_e > 10^{19} \text{ m}^{-3}$ .

power is radiated at high densities. A critical density  $\bar{n}_{e,\text{crit}} \simeq 1 \times 10^{20} \text{ m}^{-3}$  at  $B_0 = 1.5 \text{ T}$  and  $\langle\beta\rangle = 1.4\text{--}1.5\%$  at  $B_0 = 0.46\text{--}0.6 \text{ T}$  were achieved. The critical density is determined by oxygen impurity radiation; above this density  $W_{\text{dia}}$  begins to deteriorate, as for a detached plasma. Good confinement characteristics are obtained for inward-shifted magnetic axis configurations, where the configurations approach an omnigenous configuration. In high-beta plasmas, MHD activity has been observed for the inward-shifted magnetic axis configuration.

## 4.2. Plasma Physics Laboratory, Kyoto University

### 4.2.1. Heliotron E

The Heliotron E experiment [37] has been in operation since 1980. Throat-baffle plates were installed in one-fifth of the torus in a recent modification [38]. The divertor plasma parameters were unchanged by the baffles, but the neutral densities in the baffled and nonbaffled sections were different under some plasma conditions; this was consistent with theoretical predictions. A new six-pellet ( $\text{H}_2$ ,  $\text{D}_2$ ) injector has also been used.

The main objective of recent experiments [39] is to optimize the currentless, high- $\tau$ , strong-shear magnetic configuration using auxiliary toroidal and vertical field coils in order to achieve better transport and MHD stability. Changing the external toroidal field ratio  $B_{T0}/B_{H0}$  from  $-0.1$  to  $0.15$  varies  $\tau(0)$  from  $0.64$  to  $0.39$ ,  $\tau(\bar{a})$  from  $2.6$  to  $3.1$ , and  $\bar{a}$  from  $0.182 \text{ m}$  to  $0.252 \text{ m}$ . Changing the vertical field ratio  $B_{V0}/B_{H0}$  from  $-0.171$  to  $-0.199$  varies the magnetic axis shift  $\Delta_V$  from  $+0.04 \text{ m}$  to  $-0.04 \text{ m}$ . Here  $B_{T0}$ ,  $B_{H0}$ , and  $B_{V0}$  are the central magnetic fields produced by the auxiliary toroidal field coils, the helical coil, and the auxiliary vertical field coils, respectively.

The main results are as follows.

- (1) Measurements of the density profile at the plasma boundary with an electrostatic probe and a lithium beam probe show that the change of area and the position of the last magnetic surface agree well with the calculated values.
- (2) The scaling  $\tau_E \propto \bar{a}^2$  holds when  $\Delta_V \simeq -0.02 \text{ m}$  ( $B_{V0}/B_{H0} = -0.192$ ) and  $-0.1 \leq B_{T0}/B_{H0} \leq 0.1$ . The confinement is 20–50% better than that of the standard configuration, as shown in Fig. 6.
- (3) When  $\Delta_V \simeq -0.02 \text{ m}$  ( $B_{V0}/B_{H0} = -0.192$ ) and  $0.05 \leq B_{T0}/B_{H0} \leq 0.1$ , the plasma is MHD stable, although the magnetic well is very shallow in the central region. If  $\Delta_V = -0.02 \text{ m}$  and  $B_{T0}/B_{H0} = 0$ , then the plasma becomes unstable even for  $\beta(0) \sim 0.4\%$ .
- (4) For  $B_{T0}/B_{H0} = 0.05$  and  $B_{V0}/B_{H0} = -0.192$ , density clamping of an ECH plasma is overcome, and a plasma with  $T_e(0) = 350 \text{ eV}$  and  $\bar{n}_e = 3.7 \times 10^{19} \text{ m}^{-3}$ , which is higher than the rf cutoff density, can be produced in steady state without radiative collapse.

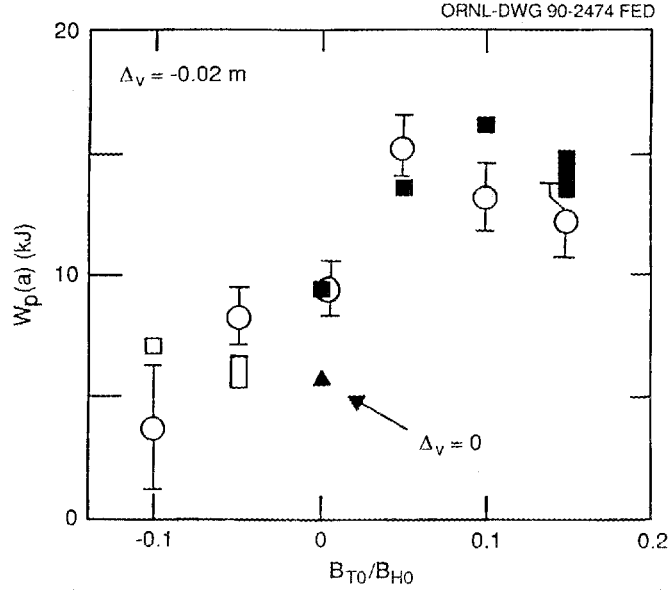


Fig. 6. The plasma energy content  $W_p(a)$  in Heliotron E is maximum for  $0.05 \lesssim B_{T0}/B_{H0} \lesssim 0.1$  and  $\Delta_V = -0.02$  m. Open circles: diamagnetic  $W_p(a)$ . Closed squares: kinetic  $W_p(a)$  at  $B = 1.90$  T. Open squares: kinetic  $W_p(a)$  at  $B = 1.76$  T.

The magnetic configuration with  $B_{T0}/B_{H0} = 0.05$ – $0.1$  and  $B_{V0}/B_{H0} = -0.192$  was found to be more favorable than the standard configuration in terms of both transport and MHD stability. Possible reasons for the improvement are (a) a reduced loss-cone configuration, (b) coincidence of drift orbits and magnetic surfaces, (c) a magnetic-well configuration, and (d) shear.

#### 4.2.2. Heliotron DR

Effects of externally applied perturbing helical fields on plasma confinement have been investigated [40] on Heliotron DR [ $R_0 = 0.9$  m,  $\bar{a} \simeq 0.07$  m,  $B_0 \lesssim 0.6$  T,  $\iota(0) = 0.8$ ,  $\iota(\bar{a}) = 2.2$ ,  $\bar{n}_e \lesssim 3 \times 10^{19}$  m $^{-3}$ ,  $T_e(0) \lesssim 400$  eV]. Two types of helical windings are used to produce a single  $m = 1$ ,  $n = 1$  magnetic island at  $r/\bar{a} \sim 0.5$  and a discrete set of magnetic islands at  $0.5 \lesssim r/\bar{a} \lesssim 1$  in overdense plasmas heated by a 28 GHz, 200 kW gyrotron at the second or third harmonic of the electron cyclotron frequency. Energy transport in these plasmas is anomalous, and the decay time of the stored plasma energy after ECH turnoff agrees with the LHD scaling law. The plasma confinement deteriorates for a perturbation field  $B_{1,1}/B_0 \gtrsim 3 \times 10^{-4}$ , which produces a large magnetic island (width  $\sim \bar{a}/4$ ) at  $r/\bar{a} \sim 0.5$ .

### 4.3. TU-Heliac (Tohoku University)

The TU-Heliac [41] has four field periods and a major radius of 0.48 m. Construction of the machine was completed in May 1988, and operation began in June of that year. Magnetic surface measurements were performed with a pulsed electron beam, and good agreement with the theoretical calculation was obtained. A pulsed microwave source (2.45 GHz, 0.5 kW) produces a plasma with a density of  $10^{13}$  to  $10^{16}$   $\text{m}^{-3}$ .

### 4.4. SHATLET-M (University of Tokyo)

A small modular-coil machine of the heliotron/torsatron type ( $\ell = 2$ ,  $M = 12$ , with a helical pitch modulation) has been filled with plasma produced by intense, pulsed  $\text{CO}_2$  laser irradiation of a tiny, free-falling deuterium pellet near the magnetic axis. The machine has  $R_0 = 0.42$  m,  $\bar{a} \simeq 0.05$  m, and  $B_0 \leq 0.15$  T [42]. Diamagnetic loop measurements show that the initial peak value of  $\langle\beta\rangle$  ranges from 3% to 5%;  $\bar{n}_e \simeq 1 \times 10^{19}$   $\text{m}^{-3}$  and  $T_i(0) \simeq 100$  eV.

### 4.5. The LHD project (National Institute for Fusion Science)

The main research activity at the new National Institute for Fusion Science (Nagoya) is the design of the LHD [43, 44]. This is a continuation of the heliotron/torsatron line developed at Kyoto University. After various field optimization studies, a heliotron/torsatron configuration with fewer field periods than Heliotron E ( $M = 10$  vs  $M = 19$ ) was chosen because of its compactness (lower aspect ratio) and better MHD stability properties. An inward shift of the magnetic axis is used to improve high-energy particle confinement and plasma confinement. The main goals of the experiment are to reach reactor-relevant parameter regimes and to explore the physics of high-temperature helical plasmas. Accordingly, the device size ( $\bar{a} \gtrsim 0.5$  m) selected is large enough to give access for powerful tangential NBI and to install a closed helical divertor, which is expected to provide enhancement of the energy confinement as well as impurity control.

This research is being carried out in collaboration with researchers at Japanese universities. Five critical physics objectives are set for the experiment:

- (1) To carry out a wide range of studies on plasma transport under high- $n\tau_E T$  plasma conditions that can be extrapolated to reactor plasmas. The closed divertor should provide H-mode-like  $\tau_E$  enhancement, as seen in tokamak divertor discharges. The target plasma parameters are  $T(0) \sim 4$  keV,  $n \sim 10^{20}$   $\text{m}^{-3}$ , and  $\tau_E \sim 0.1$  s at  $P = 20$  MW.
- (2) To achieve plasmas with  $\langle\beta\rangle \gtrsim 5\%$ , and to understand the related physics. The aim of  $\langle\beta\rangle \gtrsim 5\%$  in LHD is motivated by economic considerations for fusion reactors; thus, experimental explorations will be directed toward achieving the highest possible beta value.

- (3) To obtain the basic data necessary to realize steady-state operation through experiments on quasi-steady-state plasma control using a helical divertor. The key issue here is whether excessive impurity contamination can be prevented.
- (4) To study the behavior of high-energy particles in a helical magnetic field and to conduct  $\alpha$ -particle simulation experiments.
- (5) To increase the understanding of toroidal plasmas by carrying out studies complementary to those in tokamaks.

A sketch of LHD is shown in Fig. 7. The main device parameters are  $\ell = 2$ ,  $M = 10$ ,  $\gamma_c = 1.2$ ,  $B_0 = 4$  T,  $R_0 = 4$  m, and  $\bar{a} \gtrsim 0.5$  m. Here  $\gamma_c = M/2 \cdot a_c/R_0$  is the helical winding pitch parameter with  $a_c$  the coil radius. Other device parameters are given in Table III. The magnetic field is produced by continuous helical coils. The device parameters and the envisaged pulse duration of the plasma

ORNL-DWG 90-2475 FED

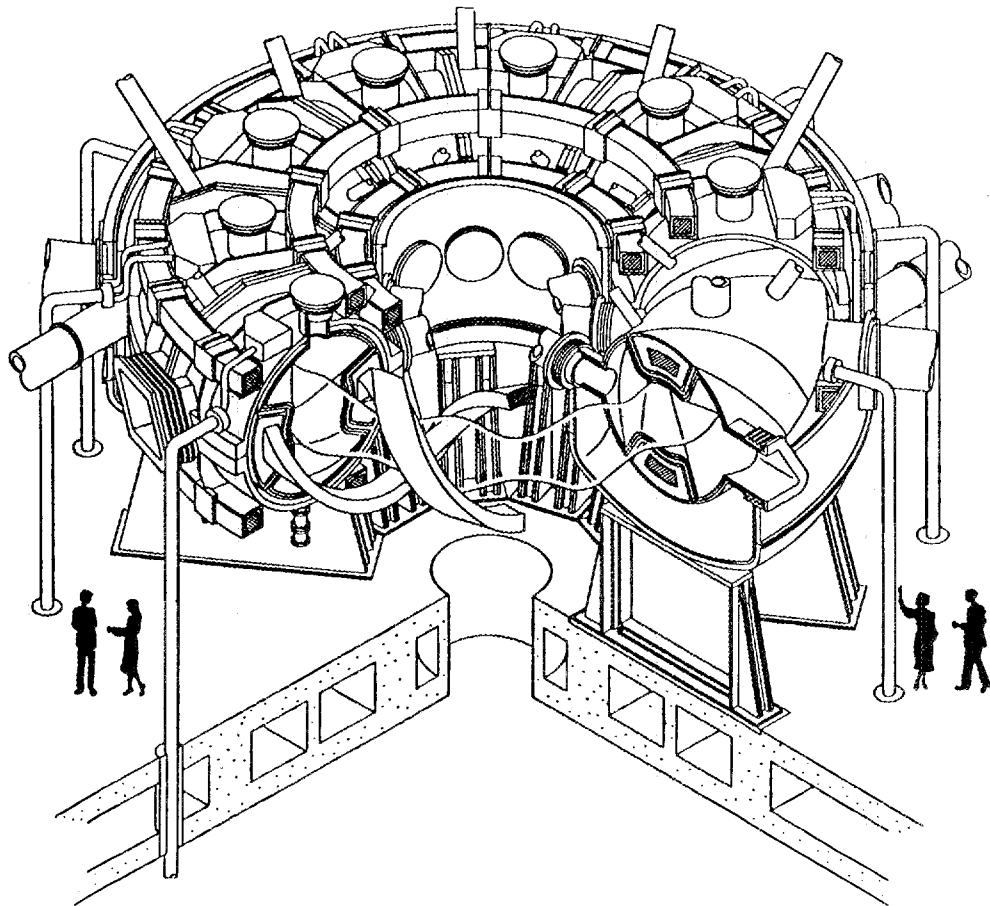


Fig. 7. Sketch of the Large Helical Device.

TABLE III. LARGE HELICAL DEVICE PARAMETERS

Plasma	
Major radius $R_0$	4 m
Average plasma radius $\bar{a}$	0.5–0.6 m
Plasma aspect ratio $R_0/\bar{a}$	7–8
Plasma volume	20–30 m <sup>3</sup>
Vacuum field	
Poloidal multipolarity $\ell$	2
Number of field periods $M$	10
Rotational transform	
At center $\iota(0)$	$\simeq 0.5$
At boundary $\iota(\bar{a})$	$\simeq 1$
Helical ripple $\epsilon_H$	$\simeq 0.2$
Magnetic field	
On axis $B_0$	4 T
At coil surface $B_{\max}$	$\simeq 8$ T
Coils	
Coil minor radius $a_c$	0.96 m
Pitch parameter $\gamma_c$	1.2
Helical coil current	8 MA·turns
Coil current density	40 MA·m <sup>-2</sup>
Number of poloidal coils	6 (3 pairs)
Magnetic energy	2 GJ
Device	
Repetition time	
For 10 s plasma duration	10 min
For 5 s plasma duration	5 min
Heating power	20 MW
Refrigeration power	5–7 kW

(10 s for  $P = 20$  MW, steady-state operation for  $P = 3$  MW) necessitate the use of superconducting coils, which is technologically relevant in considering future application to reactors.

#### 4.6. Theory and computation

Recent theoretical studies and computations have focused on the LHD project and on experimental results from CHS and Heliotron E.

(1) *MHD studies.* Computational tools for calculation of magnetic fields and MHD equilibrium and stability have been improved and used for analysis of existing experiments and for LHD design. Fairly good agreement was obtained between calculations of ideal and resistive interchange modes and experimental results from Heliotron E and Heliotron DR; the dependences of plasma confinement and MHD properties on the magnetic axis shift and the addition of a toroidal magnetic field were examined. Resistive interchange modes have been investigated theoretically. The coupling of  $\eta_i$  modes and  $g$ -modes and the effect of a radial electric field have been studied. The relationship between the Mercier criterion and low- $n$  interchange modes in a heliotron/torsatron has been clarified.

(2) *Single-particle orbit studies.* Codes have been used to follow particle orbits, and magnetic field configurations that can minimize the loss-cone region have been pursued. Finite-beta effects on the confinement of single particles have been investigated. Recently, the technique of mod- $B_{\min}$  mapping has been extended to include transition particles in realistic magnetic field configurations as well as in model fields. This allows rapid determination of configurations optimized for particle orbits.

(3) *Transport and toroidal current.* The dependences of the geometric factors for neoclassical ripple diffusion and bootstrap current on the magnetic field configuration have been examined for LHD by changing the poloidal (vertical and quadrupole) fields and the pitch modulation of the helical windings. The beam-driven (Ohkawa) current, predicted to be large for tangential NBI, has been formulated in the  $1/\nu$  regime using the drift kinetic equation. Transport codes coupled with an equilibrium code have been used to predict transport in LHD. Study of anomalous transport mechanisms indicates that the  $g$ -mode with finite-Larmor-radius effects may cause anomalous transport.

(4) *Divertor studies.* Ergodization, stochasticity, and other properties (e.g. whisker structure) of the field lines outside the confined plasma are being clarified. The connection length of field lines and the heat channel width have been studied numerically and theoretically. Divertor functions have been studied using fluid equations for the plasma and a neutral gas transport code.

(5) *Plasma heating.* Development has continued on 3-D orbit following and Monte Carlo codes for NBI in both real-space and magnetic coordinates. Ray tracing techniques have been improved to predict energy deposition by ECH in realistic 3-D configurations. Full-wave calculations have been done for the straight heliotron to predict deposition by ICH. Also, orbit following and Monte Carlo codes have been developed for ICRF minority heating.

## 5. AUSTRALIA

The Australian National University's initial involvement in stellarators started in the early 1980s, with computational studies to optimize the coil geometry for  $\ell = 3$

stellarators and to design a proposed modular device ( $R_0 = 2.1$  m,  $\bar{a} = 0.3$  m,  $\ell = 3$ ,  $B_0 \leq 3$  T), supported by development of numerical methods for helical geometry.

The heliac program started in 1984 with operation of the tabletop device SHEILA ( $R_0 = 0.2$  m,  $\bar{a} = 0.03$  m,  $B_0 \leq 0.3$  T) [45], modified in 1985 to a flexible heliac [46]. This experiment successfully demonstrated the existence of good low-beta equilibria in weakly collisional plasmas over a wide range of low-shear configurations ( $0.65 \leq \iota \leq 1.9$ ) whose geometries agree closely with vacuum field calculations. Strong resonant effects on confinement are seen at  $\iota \sim 3/2$  (inherent) and  $\iota = 1$  (due to field errors), as shown in Fig. 8 [46]. Resistive drift waves have been identified, with the measured dispersion agreeing well with a theoretical model in which the 3-D heliac geometry is transformed into a periodic cylinder

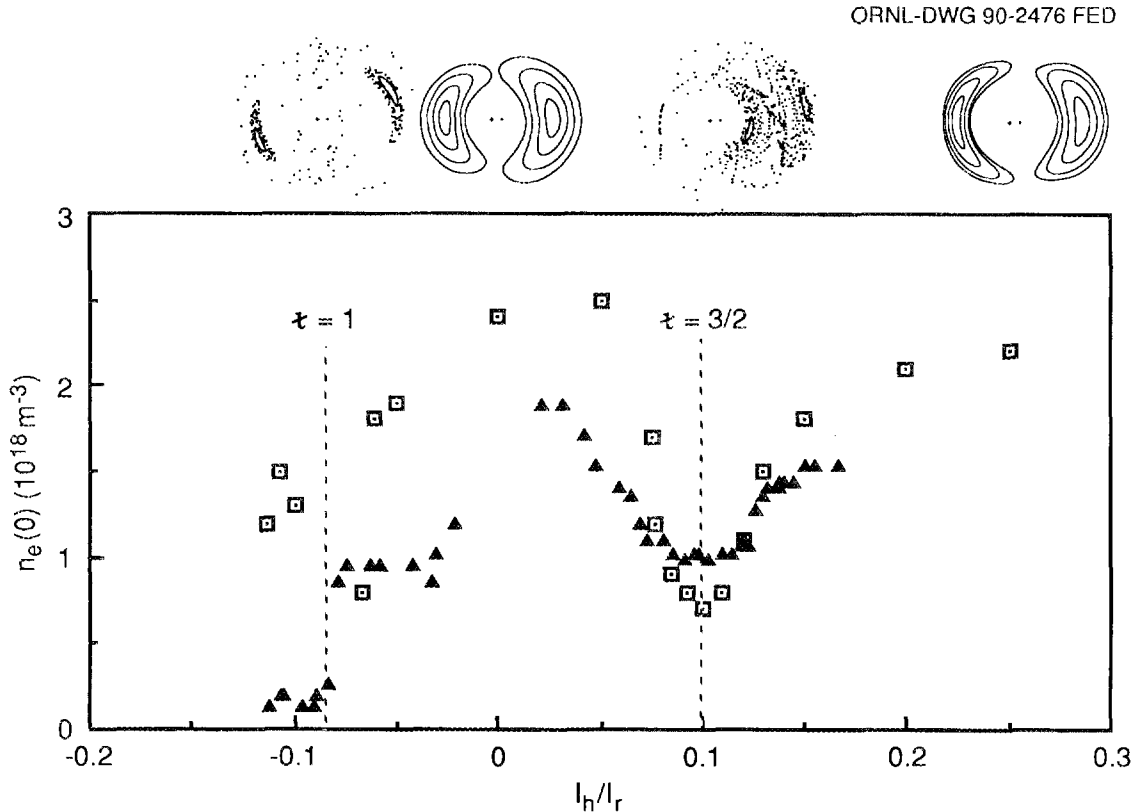


Fig. 8. The effect of low-order resonant  $\iota$  values on plasma confinement in the SHEILA heliac. The magnetic configuration (flux surface cross sections indicated above the graph) is changed by varying the ratio of the helical and poloidal coil currents,  $I_h/I_r$ . Here the dotted squares denote plasmas produced by a weak, oscillatory Ohmic discharge ( $f = 100$  kHz,  $B_0 = 0.12$  T) and the solid triangles denote plasmas produced by ECH launched from the high-field side ( $f = 2.45$  GHz,  $B_0 = 0.09$  T).

in straight-field-line magnetic coordinates [47]. New electron-beam techniques for mapping magnetic fields with very high resolution have been developed [48] and used to demonstrate accurate agreement of vacuum magnetic surfaces with calculations. Current-free plasmas have been successfully generated by a range of techniques: low-frequency, nonresonant rf (100 kHz) for  $\bar{n}_e \simeq 2 \times 10^{18} \text{ m}^{-3}$ ; whistler-wave launch ( $\bar{n}_e \gtrsim 10^{19} \text{ m}^{-3}$ ); and ECH (2.45 GHz), which produced highly overdense ( $\bar{n}_e \simeq 5 \times 10^{18} \text{ m}^{-3}$ ) plasmas when launched from the high-field side.

A much larger heliac H-1 ( $R_0 = 1 \text{ m}$ ,  $\bar{a} = 0.22 \text{ m}$ ) [49, 50] is nearing completion and is expected to operate early in 1990. It complements the Spanish four-field-period TJ-II heliac by using a small-aspect-ratio, three-field-period design, with the field variation due to the strong toroidicity reduced by modulating the toroidal field coil spacing. It is intended for basic confinement studies of low- and finite-beta plasmas over a wide range of configurations (including deep wells and magnetic hills) under more fusion-relevant conditions [ $B_0 \leq 1 \text{ T}$ ,  $T_e(0) = 200\text{--}500 \text{ eV}$ ], as well as for fundamental studies of toroidal flux surface topology under steady-state conditions (i.e., as a toroidal Q-machine) at reduced fields (0.2 T). Plasma production and heating initially will be by 200 kW ICRF power, with whistler-, fast-, and ion-Bernstein-wave launch as options and ECH as a later possibility. Special diagnostics developed through the need to derive 2-D plasma profiles in the deeply indented heliac configuration include a fast-scanning, far-infrared interferometer to provide sufficient views for tomographic inversion.

Theoretical development work has concentrated mainly on extending the Princeton PEST code to include free-boundary helical geometry and resistive modes [51–54]. Some basic work on the problem of defining optimal coordinates for configurations with imperfect surfaces is also under way [55].

Extensive 3-D MHD studies, based mainly on the ORNL VMEC and New York University BETA codes, are used to explore equilibrium over the full range of H-1 operating conditions [56]. Some of these calculations are made by the Oak Ridge group. Since the principal aim is to study the effect of configuration parameters on equilibrium and stability and on transport, these studies are used to identify the most promising experimental configurations achievable with the limited heating power available.

## 6. EUROPEAN COMMUNITY

The stellarator research program in the European Community was pursued through the early 1980s at Culham Laboratory, U.K., and the Max-Planck-Institut für Plasmaphysik (IPP), Garching, FRG, with experiments in the “classical” stellarators CLEO and Wendelstein VII-A, respectively. The major achievement in the latter machine was the first stellarator operation at substantial plasma parameters without an Ohmic heating current [57]. In the following years, the “Advanced Stellarator” line was developed at IPP Garching. The modular stellarator

Wendelstein VII-AS started operation in 1988; its next step, Wendelstein VII-X, is now being defined. When Spain joined the European Community, the fusion division of the Centro de Investigaciones Energéticas, Medioambientales, y Tecnológicas (CIEMAT) also concentrated its work on stellarators. The CIEMAT flexible heliac TJ-II has obtained EURATOM Preferential Support and is now under detailed design, and TJ-I Upgrade, a torsatron experiment with a helical magnetic axis, is under construction.

### 6.1. The TJ-II flexible heliac project

The TJ-II device [58], the cornerstone of the Spanish fusion program, is a medium-size ( $B_0 = 1$  T,  $R_0 = 1.5$  m,  $\bar{a} = 0.2$  m), four-field-period, helical-axis stellarator of the flexible heliac type. It will be built at the CIEMAT site in Madrid and is expected to operate in the second half of 1994. Addition of an  $\ell = 1$  vacuum field to the poloidal field allows effective control of the rotational transform and shear in the machine and thus generation of a wide range of magnetic configurations with high rotational transform (0.9 to 2.5), low shear ( $-1\%$  to  $10\%$ ), deep magnetic well (0 to  $6\%$ ), and average plasma radius between 0.1 m and 0.2 m, as shown in Fig. 9. This flexibility allows avoiding the most dangerous low-order resonances

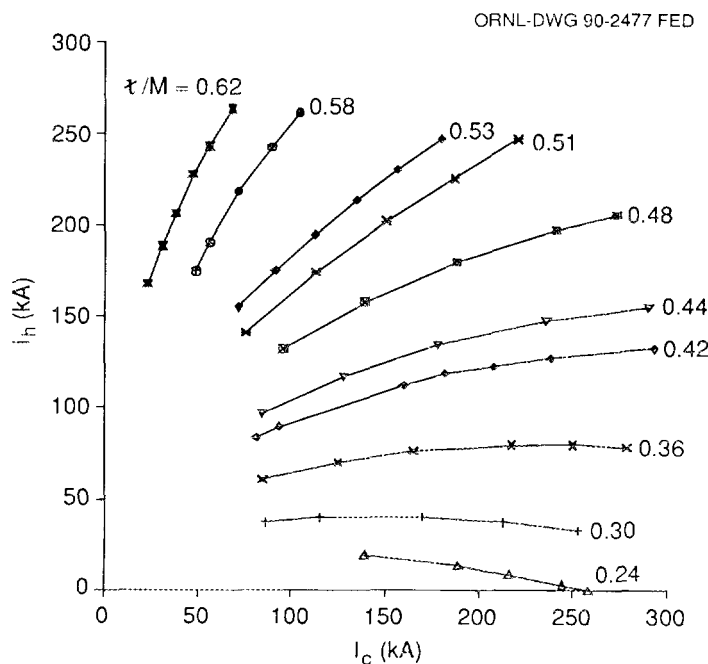


Fig. 9. Configuration flexibility ( $\tau/M$ ) obtained in the  $M = 4$  TJ-II heliac by varying the currents in the  $\ell = 1$  helical winding ( $I_h$ ) and in the circular winding ( $I_c$ ) of the linked, central toroidal coil. Each point on a curve is characterized by a different value of the magnetic well depth.

while almost independently changing the magnetic configuration parameters, thus permitting the study in one machine of the influence of the rotational transform, magnetic well, and shear on the equilibrium, stability, and transport properties of different configurations.

The first experimental stage will be dedicated to the study of low-beta phenomena. Plasma breakdown and heating will be done with two 200 kW, 53.2 GHz gyrotrons. Emphasis will be on the characterization of the equilibrium windows in the configuration space of the machine. To fully understand the high-beta potential of this heliac configuration, a second experimental phase is planned with four 1 MW tangential neutral beam lines. Calculations indicate that  $\langle\beta\rangle > 6\%$  is achievable. In this phase, special emphasis will be given to self-stabilization behavior, stability limits of the different configurations, and bootstrap current control.

The hardcore conductors of the TJ-II design are outside the vacuum chamber, which eases construction of these coils. A high degree of access to the plasma is obtained through 64 ports, as large as 0.15 m wide and 0.5 m long, located on the top, outside, and bottom of the device. This is important for diagnosing the complex 3-D configurations of TJ-II.

## 6.2. TJ-I Upgrade

TJ-I Upgrade [59] is a small, low-aspect-ratio torsatron ( $R_0 = 0.6$  m,  $\bar{a} = 0.1$  m,  $B_0 = 0.5$  T) currently under construction at CIEMAT and expected to be in operation in 1990. It is a six-field-period device with an  $\ell = 1$  coil that follows the winding law  $\phi = (\theta + 0.4 \sin \theta)/6$ . The reference magnetic configuration has  $\iota(0) = 0.3$ , a magnetic well  $\simeq 7\%$ , small shear, and a slightly helical magnetic axis. The effect of high-energy particles on plasma stability can be studied by moving the magnetic axis toward the center of the machine, eliminating the beneficial effects of the magnetic well but improving the confinement of the high-energy particles created with 200 kW, 28 GHz ECH.

## 6.3. Wendelstein VII-AS

Wendelstein VII-AS ( $R_0 = 2$  m, aspect ratio  $\simeq 10$ ) [60] is the world's largest stellarator with nonplanar modular coils. These coils produce the major part of the confining magnetic field of the Advanced Stellarator topology that is characterized by a certain reduction of the poloidal variation of  $\int dl/B$ . This improves neoclassical confinement, particle orbits, and plasma equilibrium [61]. Wendelstein VII-AS is equipped with ECH using four optimized waveguides and movable mirrors for current drive experiments [62], two neutral beam injectors with nearly tangential injection in opposite directions, and an experimental ICH antenna

operating between 30 MHz and 110 MHz; it has the potential to apply an external loop voltage. The rotational transform and magnetic axis position can be adjusted by additional toroidal and vertical fields. Extensive studies of the vacuum fields [63] have shown excellent agreement of the measured magnetic parameters with the design values.

Investigations of “currentless” ECH plasmas started in October 1988 at a reduced field of 1.25 T, using up to four gyrotrons (70 GHz,  $\leq 800$  kW) for second harmonic X-mode plasma production and heating for as long as 0.8 s. Typical plasma parameters were  $n_e(0) \leq 2 \times 10^{19} \text{ m}^{-3}$ ,  $T_e(0) \leq 2.8$  keV, and  $T_i(0) \leq 0.2$  keV at  $\iota = 0.25$ –0.65. These studies [64] allowed improving the heating efficiency, optimizing the ECH-induced current drive, and investigating the influence on the confinement of rational  $\iota$  values and on-axis vs off-axis heating (Fig. 10). The observed residual plasma current (up to a few kiloamperes, in the

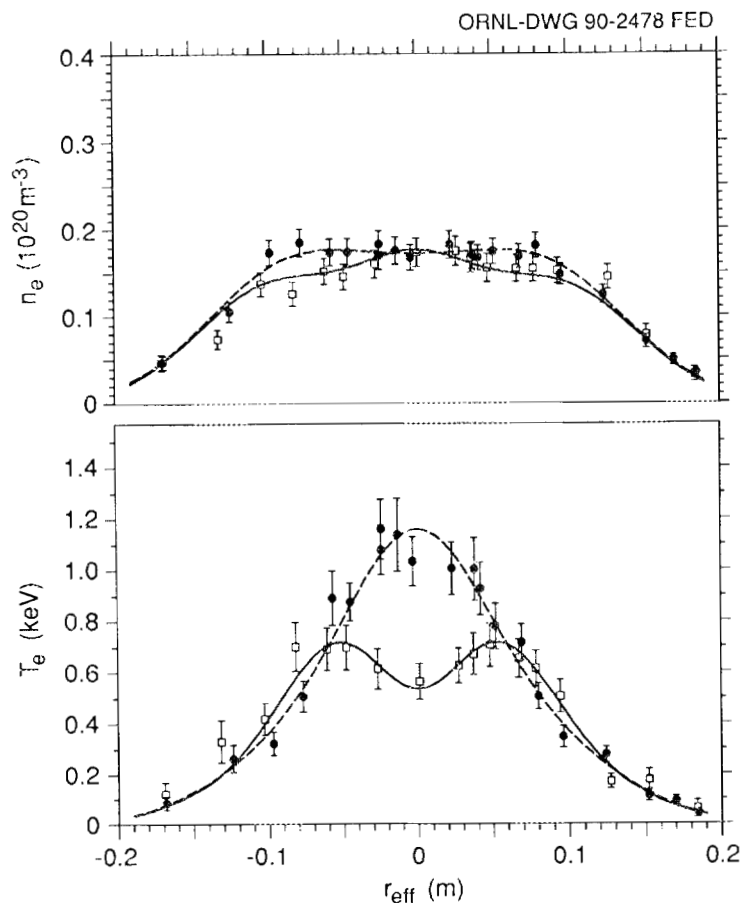


Fig. 10. Electron density and temperature profiles in Wendelstein VII-AS with 350 kW of on-axis [dashed curve,  $\iota(a) = 0.34$ ] and off-axis [solid curve,  $\iota(a) = 0.335$ ] X-mode ECH at  $B_0 = 1.26$  T.

direction and of the order of the estimated bootstrap current) is controlled by a small external loop voltage ( $V_{loop} < 0.2$  V), by  $k_{||}$  components of the applied ECH field (maximum efficiency  $20 \text{ A}\cdot\text{kW}^{-1}$ ), or by NBI current drive (up to 5 kA at 750 kW) with unbalanced injection. Preliminary ECH scoping experiments at the electron cyclotron frequency (O-mode) using two gyrotrons ( $\leq 400$  kW) yielded values of  $n_e(0) \leq 4 \times 10^{19} \text{ m}^{-3}$ ,  $T_e(0) \leq 2 \text{ keV}$ , and  $T_i(0) \leq 0.4 \text{ keV}$  for  $\tau < 0.35$ .

First analyses of the electron energy transport, charged particle balance, radiation effects, and impurity content were performed. The transport behavior is similar to the results obtained in the previous Wendelstein VII-A experiments; optimum confinement is seen in Wendelstein VII-AS if low-order rational  $\tau$  values at the plasma edge are avoided. The electron heat diffusivity  $\chi_e$  varies between  $0.5 \text{ m}^2 \cdot \text{s}^{-1}$  and  $2 \text{ m}^2 \cdot \text{s}^{-1}$  at half the minor radius, with some increase toward the center and a strong increase toward the edge; the estimated particle diffusivity is about one-tenth of the heat diffusivity [65].

Starting with an ECH-generated target plasma, discharges could be maintained by NBI alone at 1.25 T. Typical parameters were  $\bar{n}_e = 3 \times 10^{19} \text{ m}^{-3}$  and  $T_e(0) \sim T_i(0) \leq 0.3 \text{ keV}$ . The parameters could be improved with additional pellet injection. Combined ECH and NBI heating at 1.25 T was difficult because of the low cutoff density. In first tests of the ICH antenna, up to 700 kW was launched without a significant increase of density and impurities.

During September and October 1989, the support of some modular field coils was improved to reduce certain deformations of these coils observed during the short series of discharges at 2.5 T. Routine operation at the design field of 2.5 T was obtained in early 1990. ECH plasma operation gave densities up to  $4 \times 10^{19} \text{ m}^{-3}$ ,  $T_i(0) \simeq 0.4 \text{ keV}$ , and  $T_e(0)$  from 1 keV (at 170 kW) to 2.5 keV (at 700 kW);  $\tau_E \simeq 20 \text{ ms}$  at the lower power. A significant reduction in  $\chi_e$  was observed (typically  $< 1 \text{ m}^2 \cdot \text{s}^{-1}$ ) at the higher field.

#### 6.4. The Wendelstein VII-X project

The focus of the present stellarator activities at IPP Garching is the development of the large new stellarator Wendelstein VII-X [66, 67], shown in Fig. 11. This experiment is a continuation of the Advanced Stellarator line developed at IPP Garching and successfully inaugurated in Wendelstein VII-AS. A Helias configuration (Helical Advanced Stellarator) has been chosen because of its confinement and stability properties [68]. Wendelstein VII-X will go a step beyond Wendelstein VII-AS and aims to reach reactor-relevant parameter regimes with  $\langle \beta \rangle \simeq 5\%$  and to demonstrate the reactor capability of modular stellarators. For this purpose, its dimensions are large enough to give access for powerful heating and to allow the investigation of quasi-steady-state plasmas.

Wendelstein VII-X does not aim at ignition; therefore, D-T reactions will not occur, and provisions for handling radioactive materials are not needed. Effects

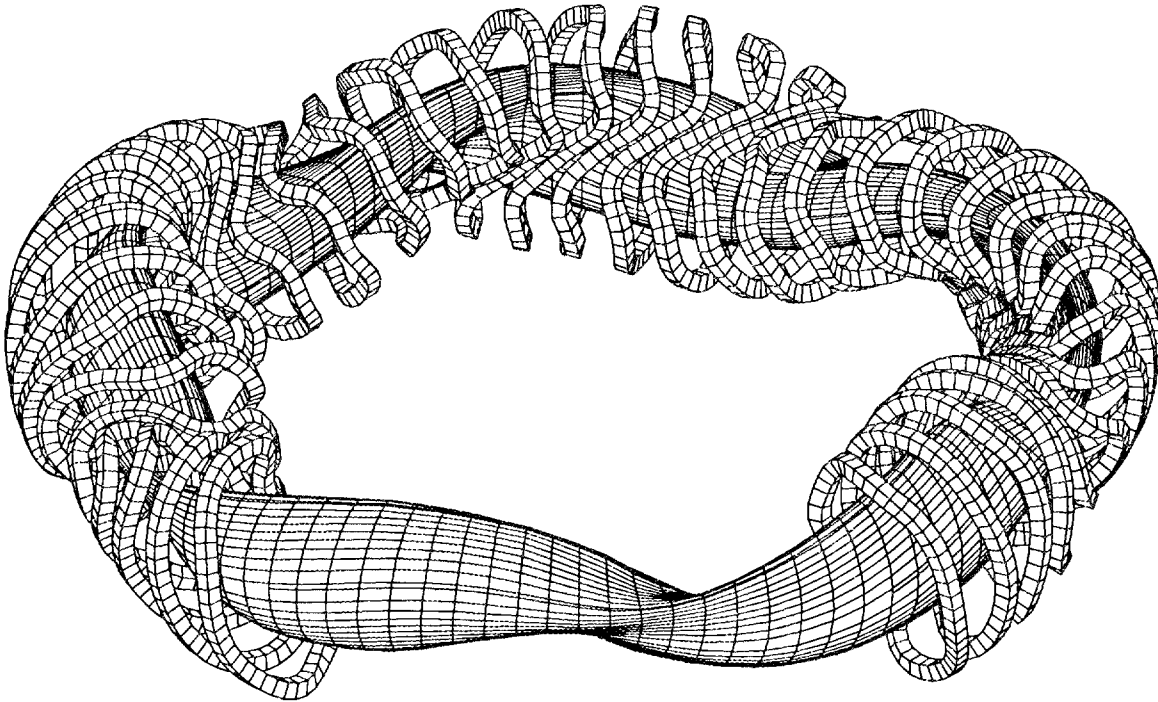


Fig. 11. Magnetic surface and nonplanar modular coils for Wendelstein VII-X (Helias 5-10). An additional system of four planar coils per period will be used for experimental flexibility.

caused by D-D neutrons play only a minor role. The temperature goal of 5 keV is determined by the fact that in a reactor this temperature regime must be reached with applied external heating; the assistance of  $\alpha$ -particle heating becomes important at higher temperatures. The temperature regime of 5 keV can be reached in Wendelstein VII-X by an effective heating power of typically 20 MW if neoclassical transport plus the anomalous transport found in the earlier Garching "classical" stellarator experiment Wendelstein VII-A prevails.

The aim of  $\langle\beta\rangle = 5\%$  in Wendelstein VII-X results mainly from economic considerations of fusion reactors: since fusion power output increases as  $\langle\beta\rangle^2$ , the limits of  $\langle\beta\rangle$ , set by plasma instabilities, must be explored experimentally and pushed as high as possible. Confinement is a critical issue facing stellarator reactors; even given the assumption of neoclassical losses, careful optimization of particle orbits and the magnetic configuration is required to reach ignition. Therefore, particular attention is given to this topic in Wendelstein VII-X. Furthermore, the bootstrap current in the long mean-free-path regime has been reduced by configuration optimization. The rotational transform and shear are chosen to avoid

low-order rational values; in addition, the coil shapes have been adjusted for small magnetic island size at higher-order resonances [69].

It is intended to produce the Wendelstein VII-X magnetic field with modular superconducting coils. This choice was made because of the envisaged pulse duration of the plasma, the available space for coils, and especially the high relevance of superconducting coils for future application to reactors. With a magnetic field of 3 T on axis and 6 T at the coils, existing NbTi technology can be used. Two study contracts with European industry have confirmed the coil feasibility. The magnetic field in Wendelstein VII-X has five field periods; other basic data [70] are  $R_0 = 5.5$  m,  $\bar{a} \simeq 0.5$  m, and stored magnetic energy  $W \simeq 0.6$  GJ (see Table IV).

TABLE IV. WENDELSTEIN VII-X PARAMETERS

Vacuum field	
Major radius $R_0$	5.5 m
Average plasma radius $\bar{a}$	0.5 m
Number of field periods $M$	5
Rotational transform	
On axis $\iota(0)$	0.84
At edge $\iota(\bar{a})$	0.99
Magnetic well depth	-1.4%
Average field on axis $B_0$	3.0 T
Coils	
Number of coils per period	10
Average coil radius $a_c$	1.14 m
Average current density	48 MA·m <sup>-2</sup>
Maximum field at coils	6.1 T
Magnetic energy	600 MJ

### 6.5. Theory

Theoretical studies of stellarator physics within the European Community cover the whole range of stellarator fields: classical stellarators, Advanced Stellarators, torsatrons, heliacs, and, especially, the innovative Helias systems, which combine elements of the Advanced Stellarator with elements of heliacs. After the end of the CLEO stellarator program at Culham Laboratory, theoretical stellarator studies were concentrated at IPP Garching. When the Spanish TJ-II project began, theoretical activities were initiated at CIEMAT, in close cooperation with ORNL and IPP Garching. Low-aspect-ratio torsatrons are also being studied at Frascati,

Italy. The aim of these studies is twofold: development of optimized stellarator topologies for application to experimental devices, and modeling and interpretation of experimental results. Analytical studies are being performed and numerical codes are being applied or developed for these purposes.

Major activities in developing optimized stellarators are in the areas of

- (1) high-quality vacuum field magnetic surfaces (including the edge structure),
- (2) good finite-beta equilibrium properties,
- (3) good MHD stability properties (resistive interchange, ideal and resistive ballooning, global modes),
- (4) small neoclassical transport in the  $1/\nu$  regime,
- (5) small bootstrap current in the long mean-free-path regime,
- (6) good collisionless  $\alpha$ -particle containment,
- (7) good modular coil feasibility,
- (8) plasma heating (neutral beam deposition, ECH ray tracing),
- (9) neutral particle transport and recycling,
- (10) error fields and perturbations.

Theoretical activities in interpretation of experimental results as well as predictive modeling of plasma behavior include plasma diagnostics (spectroscopy, soft X-rays, bolometry, magnetic diagnostics, etc.), profile analyses including finite-beta effects (transformation of spatial to magnetic coordinates), studies of transport (global scaling or local dependences, including anomalous losses) for charged and neutral particles, and edge effects.

Results of these investigations are summarized in Ref. [1] for the period 1981 to 1986; a number of recent new theoretical investigations in the European Community are described in Refs. [71] and [72]. In the field of reactor studies, critical issues of Advanced Stellarators, upgraded to “burner” and reactor systems, were studied in Ref. [73].

## 7. SUMMARY

Significant values of plasma parameters have been obtained in ATF, CHS, Heliotron E, and the Wendelstein stellarators. Among important achievements are the attainment of “currentless” plasmas with substantial stored energy using NBI, operation up to the beta limit of resistive interchange modes, and, more recently, attainment of the second stability regime. Electron heat conduction approaching neoclassical values has been seen in certain experiments near the center; toward the edge, anomalous losses are found. For present device parameters, global electron energy confinement times are described by an empirical relationship with some degradation at increased heating power. Neoclassical values for ion heat conduction and bootstrap current have been reported.

Stellarators lag behind current tokamak experiments by one to two machine generations, if one compares machine size and auxiliary heating power. The physics understanding of stellarators is now advanced enough to proceed to a new generation of hydrogen experiments with reactor-relevant parameters. Three large next-generation machines that are under design or in the development stage should be more competitive with current tokamak experiments and feature the ability to operate in true steady-state fashion with superconducting coils.

Although separate national programs are described in this paper, there is strong international cooperation in the field of stellarator research. In view of the variety of stellarator topologies, an intense interaction and exchange of personnel and information are indispensable. Joint activities of the various institutes include scientific personnel visits and participation in experiments, as well as the development, exchange, and utilization of computer codes, diagnostic methods, equipment, etc. Individually, the separate programs will establish the relative importance of the optimization principles in the different stellarator approaches; together, they will produce a data base from which it should be possible to draw conclusions on an optimal stellarator configuration for an economical steady-state fusion reactor.

#### ACKNOWLEDGMENTS

The authors acknowledge contributions to this paper by a number of their colleagues: for Section 2, D. T. Anderson, R. F. Gandy, J. Johnson, M. Murakami, B. A. Nelson; for Section 4, M. Katsurai, K. Matsuoka, O. Motojima, T. Obiki, M. Okamoto, M. Wakatani, H. Watanabe; and for Section 6, J. Nührenberg, H. Renner, H. Wobig.

## REFERENCES

- [1] CARRERAS, B.A., GRIEGER, G., HARRIS, J.H., et al., Nucl. Fusion **28** (1988) 1613.
- [2] KOVRIZHNYKH, L.M., Plasma Phys. Controlled Fusion **30** (1988) 67.
- [3] LYON, J.F., Fusion Technol. **17** (1990) 19.
- [4] LYON, J.F., CARRERAS, B.A., CHIPLEY, K.K., et al., Fusion Technol. **10** (1986) 179.
- [5] LYON, J.F., BELL, G.L., BELL, J.D., et al, Fusion Technol. **17** (1990) 33.
- [6] HARRIS, J.H., MURAKAMI, M., CARRERAS, B.A., et al., Phys. Rev. Lett. **63** (1989) 1249.
- [7] MURAKAMI, M., ANABITARTE, E., ANDERSON, F.S.B., et al., Overview of Recent Results from the Advanced Toroidal Facility, ORNL/TM-11453, Oak Ridge National Laboratory, Oak Ridge, TN (1990).
- [8] SUDO, S., TAKEIRI, Y., ZUSHI, H., et al., Nucl. Fusion **30** (1990) 11.
- [9] HIDALGO, C., UCKAN, T., BELL, J.D., et al., Edge turbulence studies in ATF, in Controlled Fusion and Plasma Physics (Proc. 17th Eur. Conf. Amsterdam, 1990), to be published by the European Physical Society (1990).
- [10] DOERNER, R.P., ANDERSON, D.T., ANDERSON, F.S.B., PROBERT, P.H., SHOHET, J.L., TALMADGE, J.N., Phys. Fluids **29** (1986) 3807.
- [11] TALMADGE, J.N., ANDERSON, D.T., Nucl. Fusion **28** (1988) 1879.
- [12] TALMADGE, J.N., STORLIE, C.A., ANDERSON, D.T., et al., Nucl. Fusion **29** (1989) 1806.
- [13] LYON, J.F., CARRERAS, B.A., DOMINGUEZ, N., et al., Fusion Technol. **17** (1990) 188.
- [14] LYON, J.F., CARRERAS, B.A., LYNCH, V.E., TOLLIVER, J.S., SVIATOSLAVSKY, I.N., Fusion Technol. **15** (1989) 1401.
- [15] PAINTER, S.L., LYON, J.F., Fusion Technol. **16** (1989) 157.
- [16] Proceedings of the 7th International Workshop on Stellarators (Oak Ridge, 1989), IAEA-TECDOC-XXXX, IAEA, Vienna (1990).
- [17] BYKOV, V.E., VOLKOV, E.D., VOITSENYA, V.S., et al., Magnetic field configuration of the modified Uragan-3M torsatron, in Proceedings of the 7th International Workshop on Stellarators (Oak Ridge, 1989), IAEA-TECDOC-XXXX, IAEA, Vienna (1990).
- [18] BEREZHNYI, V.L., VASIL'EV, M.P., VOITSENYA, V.S., et al., Power balance studies for RF heated plasma in the Uragan-3 torsatron, in Proceedings of the 7th International Workshop on Stellarators (Oak Ridge, 1989), IAEA-TECDOC-XXXX, IAEA, Vienna (1990).
- [19] VASIL'EV, V.V., VOITSENYA, V.S., VOLKOV, E.D., et al., Impurity studies for the RF heated plasma in the Uragan-3 torsatron, in Proceedings of the 7th International Workshop on Stellarators (Oak Ridge, 1989), IAEA-TECDOC-XXXX, IAEA, Vienna (1990).

- [20] BEREZHNYI, V.I., BESEDIN, N.T., VASIL'EV, M.P., et al., in Plasma Physics and Controlled Nuclear Fusion Research 1986 (Proc. 11th Int. Conf. Kyoto, 1986), Vol. 2, IAEA, Vienna (1987) 497.
- [21] BYKOV, V.E., GEORGIEVSKIJ, A.V., DEMCHENKO, V.V., et al., Fusion Technol. **17** (1990) 140.
- [22] SHISHKIN, A.A., Vopr. At. Nauki Tekh. Ser. Termoyadernyi Sintez **2** (1987) 15.
- [23] SHISHKIN, A.A., BYKOV, V.E., PELETMINSKAYA, V.G., KHODY-ACHIKH, A.V., in Controlled Fusion and Plasma Physics (Proc. 15th Eur. Conf. Dubrovnik, 1988), Vol. 12B, Part 2, European Physical Society (1988) 478.
- [24] BYKOV, V.E., GREKOV, D.L., SHISHKIN, A.A., GARCIA, L., HARRIS, J.H., ROME, J.A., Nucl. Fusion **28** (1988) 871.
- [25] BEIDLER, C.D., HITCHON, W.N.G., GREKOV, D.L., SHISHKIN, A.A., Nucl. Fusion **30** (1990) 405.
- [26] ANDRYUKHINA, E. D., BEREZHETSKIJ, M.S., et al., Stellarator L-2, Preprint N 154, P.N. Lebedev Institute, Moscow (1977).
- [27] ANDRYUKHINA, E.D., BATANOV, G.M., BEREZHETSKII, M.S., et al., in Controlled Fusion and Plasma Physics (Proc. 12th Eur. Conf. Budapest, 1985), Vol. 9F, Part 1, European Physical Society (1985) 421.
- [28] L-2 TEAM and ECR GROUP, Plasma Phys. Controlled Fusion **31** (1989) 1705.
- [29] BATANOV, G.M., KOLIK, L.V., SAPOZHNIKOV, A.V., SARKSYAN, K.A., KHOL'NOV, Yu.V., SHATS, M.G., in Controlled Fusion and Plasma Physics (Proc. 15th Eur. Conf. Dubrovnik, 1988), Vol. 12B, Part 2, European Physical Society (1988) 455.
- [30] KOVRIZHNYKH, L.M., SHASHARINA, S.G., Nucl. Fusion **30** (1990) 453.
- [31] KOVRIZHNYKH, L.M., SHASHARINA, S.G., Comments Plasma Phys. Controlled Fusion **12** (1989) 305.
- [32] SYCHUGOV, D.Yu., SHCHEPETOV, S.V., Sov. J. Plasma Phys. **14** (1988) 390; KOVRIZHNYKH, L.M., KOSTOMAROV, D.P., SYCHUDOV, D.Yu., SHCHEPETOV, S.V., Differentsialnyje Uravnenia **25** (1989) 983.
- [33] DANILKIN, I.S., KOVRIZHNYKH, L.M., MINEEV, A.B., KHADIN, O.E., SPIEGEL, I.S., Choice of a stellarator configuration with reduced neoclassical losses (in Russian), Preprint No. 51, General Physics Institute, Moscow (1989).
- [34] DANILKIN, I.S., KOVRIZHNYKH, L.M., KOMIN, A.B., et al., Vopr. At. Nauki Tekh. Ser. Termoyadernyi Sintez **3** (1987) 3.
- [35] NISHIMURA, K., MATSUOKA, K., FUJIWARA, M., et al., Fusion Technol. **17** (1990) 86.
- [36] MATSUOKA, K., CHS GROUP, in Proc. 1st Int. Toki Conf. Plasma Physics and Controlled Nuclear Fusion (Toki, 1989), NIFS-PROC-3, National Institute for Fusion Science, Nagoya (1990) 93.

- [37] MOTOJIMA, O., IYOSHI, A., UO, K., in Proc. 8th Symp. on Engineering Problems of Fusion Research (San Francisco, 1979), Vol. II, IEEE, New York (1979) 789.
- [38] OBIKI, T., WAKATANI, M., SATO, M., et al., Fusion Technol. **17** (1990) 101.
- [39] OBIKI, T., WAKATANI, M., SANNO, F., et al., in Proc. 1st Int. Toki Conf. Plasma Physics and Controlled Nuclear Fusion (Toki, 1989), NIFS-PROC-3, National Institute for Fusion Science, Nagoya (1990) 89.
- [40] MORIMOTO, S., NAKASUGA, M., YANAGI, N., SATO, M., OBIKI, T., in Proc. 1st Int. Toki Conf. Plasma Physics and Controlled Nuclear Fusion (Toki, 1989), NIFS-PROC-3, National Institute for Fusion Science, Nagoya (1990) 73.
- [41] KITAJIMA, S., TAKAYAMA, M., ZAMA, T., TAKEUCHI, N., WATANABE, H., in Proc. 1st Int. Toki Conf. Plasma Physics and Controlled Nuclear Fusion (Toki, 1989), NIFS-PROC-3, National Institute for Fusion Science, Nagoya (1990) 97.
- [42] SEKI, H., OHSAKI, H., OKUYAMA, H., et al., in Plasma Physics and Controlled Nuclear Fusion Research 1988 (Proc. 12th Int. Conf. Nice, 1988), Vol. 2, IAEA, Vienna (1989) 645.
- [43] IYOSHI, A., FUJIWARA, M., MOTOJIMA, O., OHYABU, N., YAMAZAKI, K., Fusion Technol. **17** (1990) 169.
- [44] MOTOJIMA, O., LHD DESIGN GROUP, in Proc. 1st Int. Toki Conf. Plasma Physics and Controlled Nuclear Fusion (Toki, 1989), NIFS-PROC-3, National Institute for Fusion Science, Nagoya (1990) 3.
- [45] BLACKWELL, B.D., HAMBERGER, S.M., SHARP, L.E., SHI, X.H., Nucl. Fusion **25** (1985) 1485.
- [46] SHI, X.H., HAMBERGER, S.M., BLACKWELL, B.D., Nucl. Fusion **28** (1988) 259; see also BLACKWELL, B.D., HAMBERGER, S.M., SHARP, L.E., SHI, X.H., Aust. J. Phys. **42** (1989) 73.
- [47] SHI, X.H., BLACKWELL, B.D., HAMBERGER, S.M., Plasma Phys. Controlled Fusion Res. **31** (1989) 2011.
- [48] TOU, T.Y., BLACKWELL, B.D., SHARP, L.E., Magnetic field mapping using an image intensifying fluorescent probe, to be published in Rev. Sci. Instrum.
- [49] HAMBERGER, S.M., BLACKWELL, B.D., SHARP, L.E., SHENTON, D.B., Fusion Technol. **17** (1990) 123.
- [50] BLACKWELL, B.D., DEWAR, R.L., GARDNER, H.J., et al., in Plasma Physics and Controlled Nuclear Fusion Research 1986 (Proc. 11th Int. Conf. Kyoto, 1986), Vol. 2, IAEA, Vienna (1987) 511.
- [51] GARDNER, H.J., DEWAR, R.L., SY, W.N.-C., J. Comput. Phys. **74** (1988) 477.
- [52] DEWAR, R.L., GARDNER, H.J., J. Comput. Phys. **77** (1988) 485.

- [53] COOPER, G.J., Stability of Helical Plasmas, Ph.D. Thesis, The Australian National University, Canberra (1989).
- [54] DEWAR, R.L., PLETZER, A., Two dimensional generalizations of the Newcomb equation, to be published in *J. Plasma Phys.*
- [55] DEWAR, R.L., *Physica* **17D** (1985) 37.
- [56] DEWAR, R.L., GARDNER, H.J., COOPER, G.J., et al., in Proc. 1st Int. Toki Conf. Plasma Physics and Controlled Nuclear Fusion (Toki, 1989), NIFS-PROC-3, National Institute for Fusion Science, Nagoya (1990) 17.
- [57] W VII-A TEAM, NEUTRAL INJECTION TEAM, in Plasma Physics and Controlled Nuclear Fusion Research 1980 (Proc. 8th Int. Conf. Brussels, 1980), Vol. 1, IAEA, Vienna (1981) 185.
- [58] ALEJALDRE, C., ALONSO, J., BOTIJA, J., et al., *Fusion Technol.* **17** (1990) 131.
- [59] NAVARRO, A.P., GUASP, J., ALEJALDRE, C., et al., in Proc. 1st Int. Toki Conf. Plasma Physics and Controlled Nuclear Fusion (Toki, 1989), NIFS-PROC-3, National Institute for Fusion Science, Nagoya (1990) 117.
- [60] SAPPER, J., RENNER, H., *Fusion Technol.* **17** (1990) 62.
- [61] BROSSMANN, U., DOMMASCHK, W., HERRNEGGER, F., et al., in Plasma Physics and Controlled Nuclear Fusion Research 1982 (Proc. 9th Int. Conf. Baltimore, 1982), Vol. 3, IAEA, Vienna (1983) 141.
- [62] ERCKMANN, V., WENDELSTEIN VII-AS TEAM, KASPAREK, W., MÜLLER, G.A., SCHÜLLER, P.G., THUMM, M., *Fusion Technol.* **17** (1990) 76.
- [63] JAENICKE, R., SCHWÖRER, K., ASCASIBAR, E., et al., in Controlled Fusion and Plasma Physics (Proc. 16th Eur. Conf. Venice, 1989), Vol. 13B, Part 2, European Physical Society (1989) 627.
- [64] RINGLER, H., W VII-AS TEAM, NBI-GROUP, ICF-GROUP, ECRH-GROUP, in Proc. 1st Int. Toki Conf. Plasma Physics and Controlled Nuclear Fusion (Toki, 1989), NIFS-PROC-3, National Institute for Fusion Science, Nagoya (1990) 81.
- [65] RENNER, H., W7AS TEAM, NBI GROUP, ICF GROUP, ECRH GROUP, *Plasma Physics Controlled Fusion* **31** (1989) 1579.
- [66] GRIEGER, G., BEIDLER, C., HARMEYER, E., et al., in Plasma Physics and Controlled Nuclear Fusion Research (Proc. 12th Int. Conf. Nice, 1988), Vol. 2, IAEA, Vienna (1989) 369.
- [67] BEIDLER, C., GRIEGER, G., HERRNEGGER, F., et al., *Fusion Technol.* **17** (1990) 148.
- [68] NÜHRENBERG, J., ZILLE, R., *Physics Letters A* **144** (1986) 129.
- [69] RAU, F. (editor), Proc. 3rd Workshop on Wendelstein VII-X (Schloss Ringberg, 1989), Rep. IPP-2/302, Max-Planck-Institut für Plasmaphysik, Garching (1989).

- [70] GRIEGER, G., W VII-X TEAM, in Proc. 1st Int. Toki Conf. Plasma Physics and Controlled Nuclear Fusion (Toki, 1989), NIFS-PROC-3, National Institute for Fusion Science, Nagoya (1990) 7.
- [71] Fourteen papers in Controlled Fusion and Plasma Physics (Proc. 16th European Conf. Venice, 1989), Vol. 13B, Part 2, European Physical Society (1989) 579–699.
- [72] Five papers in Proc. 1st Int. Toki Conf. Plasma Physics and Controlled Nuclear Fusion (Toki, 1989), NIFS-PROC-3, National Institute for Fusion Science, Nagoya (1990).
- [73] Five papers in Fusion Reactor Design and Technology (Proc. 4th IAEA Tech. Committee Mtg. Yalta, 1986), IAEA, Vienna (1987); see also BÖHME, G., EL-GUEBALY, L.A., EMMERT, G.A., et al., Studies of a Modular Advanced Stellarator Reactor ASRA6C, Rep. IPP-2/285, Max-Planck-Institut für Plasmaphysik, Garching (1987).

**INTERNAL DISTRIBUTION**

- |                        |                                      |
|------------------------|--------------------------------------|
| 1. C. C. Baker         | 23. G. H. Neilson                    |
| 2. L. A. Berry         | 24. B. E. Nelson                     |
| 3. B. A. Carreras      | 25. Y-K. M. Peng                     |
| 4. R. A. Dory          | 26. J. A. Rome                       |
| 5. J. L. Dunlap        | 27. M. J. Saltmarsh                  |
| 6. R. H. Fowler        | 28. T. E. Shannon                    |
| 7. W. Fulkerson        | 29. D. W. Swain                      |
| 8. J. H. Harris        | 30. N. A. Uckan                      |
| 9. H. H. Haselton      | 31. J. Sheffield                     |
| 10. C. L. Hedrick      | 32-33. Laboratory Records Department |
| 11. S. P. Hirshman     | 34. Laboratory Records, ORNL-RC      |
| 12. J. T. Hogan        | 35. Central Research Library         |
| 13. R. C. Isler        | 36. Document Reference Section       |
| 14. R. L. Johnson      | 37. Fusion Energy Division Library   |
| 15. M. S. Lubell       | 38-39. ET/FE Division                |
| 16-20. J. F. Lyon      | Publications Office                  |
| 21. P. K. Mioduszewski | 40. ORNL Patent Office               |
| 22. M. Murakami        |                                      |

**EXTERNAL DISTRIBUTION**

41. Office of the Assistant Manager for Energy Research and Development, U.S. Department of Energy, Oak Ridge Operations Office, P. O. Box E, Oak Ridge, TN 37831
42. J. D. Callen, Department of Nuclear Engineering, University of Wisconsin, Madison, WI 53706-1687
43. R. W. Conn, Department of Chemical, Nuclear, and Thermal Engineering, University of California, Los Angeles, CA 90024
44. N. A. Davies, Acting Director, Office of Fusion Energy, Office of Energy Research, ER-50 Germantown, U.S. Department of Energy, Washington, DC 20545
45. S. O. Dean, Fusion Power Associates, Inc., 2 Professional Drive, Suite 248, Gaithersburg, MD 20879
46. H. K. Forsen, Bechtel Group, Inc., Research Engineering, P. O. Box 3965, San Francisco, CA 94119
47. J. R. Gilleland, L-644, Lawrence Livermore National Laboratory, P.O. Box 5511, Livermore, CA 94550

48. R. W. Gould, Department of Applied Physics, California Institute of Technology, Pasadena, CA 91125
49. R. A. Gross, Plasma Research Laboratory, Columbia University, New York, NY 10027
50. D. M. Meade, Princeton Plasma Physics Laboratory, P.O. Box 451, Princeton, NJ 08543
51. M. Roberts, International Programs, Office of Fusion Energy, Office of Energy Research, ER-52 Germantown, U.S. Department of Energy, Washington, DC 20545
52. W. M. Stacey, School of Nuclear Engineering and Health Physics, Georgia Institute of Technology, Atlanta, GA 30332
53. D. Steiner, Nuclear Engineering Department, NES Building, Tibbetts Avenue, Rensselaer Polytechnic Institute, Troy, NY 12181
54. R. Varma, Physical Research Laboratory, Navrangpura, Ahmedabad 380009, India
55. Bibliothek, Max-Planck Institut für Plasmaphysik, Boltzmannstrasse 2, D-8046 Garching, Federal Republic of Germany
56. Bibliothek, Institut für Plasmaphysik, KFA Jülich GmbH, Postfach 1913, D-5170 Jülich, Federal Republic of Germany
57. Bibliothek, KfK Karlsruhe GmbH, Postfach 3640, D-7500 Karlsruhe 1, Federal Republic of Germany
58. Bibliotheque, Centre de Recherches en Physique des Plasmas, Ecole Polytechnique Fédérale de Lausanne, 21 Avenue des Bains, CH-1007 Lausanne, Switzerland
59. R. Aymar, CEN/Cadarache, Departement de Recherches sur la Fusion Contrôlée, F-13108 Saint-Paul-lez-Durance Cedex, France
60. Bibliothèque, CEN/Cadarache, F-13108 Saint-Paul-lez-Durance Cedex, France
61. Library, Culham Laboratory, UKAEA, Abingdon, Oxfordshire, OX14 3DB, England
62. Library, JET Joint Undertaking, Abingdon, Oxfordshire OX14 3EA, England
63. Library, FOM-Instituut voor Plasmafysica, Rijnhuizen, Edisonbaan 14, 3439 MN Nieuwegein, The Netherlands
64. Library, National Institute for Fusion Science, Chikusa-ku, Nagoya 464-01, Japan
65. Library, International Centre for Theoretical Physics, P.O. Box 586, I-34100 Trieste, Italy
66. Library, Centro Richerche Energia Frascati, C.P. 65, I-00044 Frascati (Roma), Italy
67. Library, Plasma Physics Laboratory, Kyoto University, Gokasho, Uji, Kyoto 611, Japan
68. Plasma Research Laboratory, Australian National University, P.O. Box 4, Canberra, A.C.T. 2601, Australia

69. Library, Japan Atomic Energy Research Institute, Naka Fusion Research Establishment, 801-1 Mukoyama, Naka-machi, Naka-gun, Ibaraki-ken, Japan
70. G. A. Eliseev, I. V. Kurchatov Institute of Atomic Energy, P. O. Box 3402, 123182 Moscow, U.S.S.R.
71. V. A. Glukhikh, Scientific-Research Institute of Electro-Physical Apparatus, 188631 Leningrad, U.S.S.R.
72. I. Shpigel, Institute of General Physics, U.S.S.R. Academy of Sciences, Ulitsa Vavilova 38, Moscow, U.S.S.R.
73. D. D. Ryutov, Institute of Nuclear Physics, Siberian Branch of the Academy of Sciences of the U.S.S.R., Sovetskaya St. 5, 630090 Novosibirsk, U.S.S.R.
74. O. S. Pavlichenko, Kharkov Physical-Technical Institute, Academical St. 1, 310108 Kharkov, U.S.S.R.
75. Deputy Director, Southwestern Institute of Physics, P.O. Box 15, Leshan, Sichuan, China (PRC)
76. Director, The Institute of Plasma Physics, P.O. Box 26, Hefei, Anhui, China (PRC)
77. R. A. Blanken, Experimental Plasma Research Branch, Division of Applied Plasma Physics, Office of Fusion Energy, Office of Energy Research, ER-542, Germantown, U.S. Department of Energy, Washington, DC 20545
78. R. A. E. Bolton, IREQ Hydro-Quebec Research Institute, 1800 Montee Ste-Julie, Varennes, P.Q. JOL 2P0, Canada
79. D. H. Crandall, Division of Applied Plasma Physics, Office of Fusion Energy, Office of Energy Research, ER-542, Germantown, U.S. Department of Energy, Washington, DC 20545
80. R. L. Freeman, General Atomics, P.O. Box 85608, San Diego, CA 92138-5608
81. K. W. Gentle, RLM 11.222, Institute for Fusion Studies, University of Texas, Austin, TX 78712
82. R. J. Goldston, Princeton Plasma Physics Laboratory, P.O. Box 451, Princeton, NJ 08543
83. J. C. Hosea, Princeton Plasma Physics Laboratory, P.O. Box 451, Princeton, NJ 08543
84. R. Dagazian, Division of Confinement Systems, Office of Fusion Energy, Office of Energy Research, ER-55, Germantown, U.S. Department of Energy, Washington, DC 20545
85. R. H. McKnight, Experimental Plasma Research Branch, Division of Applied Plasma Physics, Office of Fusion Energy, Office of Energy Research, ER-542, Germantown, U.S. Department of Energy, Washington, DC 20545
86. E. Oktay, Division of Confinement Systems, Office of Fusion Energy, Office of Energy Research, ER-55, Germantown, U.S. Department of Energy, Washington, DC 20545
87. D. Overskei, General Atomics, P.O. Box 85608, San Diego, CA 92138-5608
88. R. R. Parker, Plasma Fusion Center, NW 16-288, Massachusetts Institute of Technology, Cambridge, MA 02139

89. W. L. Sadowski, Fusion Theory and Computer Services Branch, Division of Applied Plasma Physics, Office of Fusion Energy, Office of Energy Research, ER-541, Germantown, U.S. Department of Energy, Washington, DC 20545
90. J. W. Willis, Division of Confinement Systems, Office of Fusion Energy, Office of Energy Research, ER-55, Germantown, U.S. Department of Energy, Washington, DC 20545
91. A. P. Navarro, Division de Fusion, CIEMAT, Avenida Complutense 22, E-28040 Madrid, Spain
92. Laboratory for Plasma and Fusion Studies, Department of Nuclear Engineering, Seoul National University, Shinrim-dong, Gwanak-ku, Seoul 151, Korea
93. J. L. Johnson, Plasma Physics Laboratory, Princeton University, P.O. Box 451, Princeton, NJ 08543
94. L. M. Kovrizhnykh, Institute of General Physics, U.S.S.R. Academy of Sciences, Ulitsa Vavilova 38, 117924 Moscow, U.S.S.R.
95. T. Obiki, Plasma Physics Laboratory, Kyoto University, Gokasho, Uji, Kyoto, Japan
96. A. Iiyoshi, National Institute for Fusion Science, Chikusa-ku, Nagoya 464-01, Japan
97. V. D. Shafranov, I. V. Kurchatov Institute of Atomic Energy, P.O. Box 3402, 123182 Moscow, U.S.S.R.
98. J. L. Shohet, Torsatron/Stellarator Laboratory, University of Wisconsin, Madison, WI 53706
99. G. Grieger, Max-Planck Institut für Plasmaphysik, D-8046 Garching, Federal Republic of Germany
100. K. Matsuoka, National Institute for Fusion Science, Chikusa-ku, Nagoya 464-01, Japan
101. F. L. Ribe, University of Washington, Aerospace and Energetics Research Program, Mail Stop FL-10, Seattle, WA 98915
102. D. G. Swanson, Auburn University, Department of Physics, Auburn, AL 36849
103. R. K. Linford, Los Alamos National Laboratory, MS F646, P.O. Box 1663, Los Alamos, NM 87545
104. K. I. Thomassen, L-637, Lawrence Livermore National Laboratory, P.O. Box 5511, Livermore, CA 94550
105. R. F. Gandy, Physics Department, Auburn University, Auburn, AL 36849
106. F. Rau, Max Planck Institut für Plasmaphysik, D-8046 Garching, Federal Republic of Germany
107. S. M. Hamberger, Plasma Research Laboratory, Australian National University, P.O. Box 4, Canberra, A.C.T. 2601, Australia
- 108-157. Given distribution as shown in OSTI-4500, Magnetic Fusion Energy (Category Distribution UC-426)